Circulation Research
JOURNAL OF THE AMERICAN HEART ASSOCIATION

American Heart Association®
Learn and Live℠

Enzymatic Single-Chain Antibody Tagging : A Universal Approach to Targeted Molecular Imaging and Cell Homing in Cardiovascular Disease

H.T. Ta, S. Prabhu, E. Leitner, F. Jia, D. von Elverfeldt, Katherine E. Jackson, T. Heidt, A.K.N. Nair, H. Pearce, C. von zur Muhlen, X. Wang, K. Peter and C.E. Hagemeyer

Circulation Research 2011, 109:365-373: originally published online June 23, 2011
doi: 10.1161/CIRCRESAHA.111.249375
Circulation Research is published by the American Heart Association. 7272 Greenville Avenue, Dallas, TX 72514
 Print ISSN: 0009-7330. Online ISSN: 1524-4571

Enzymatic Single-Chain Antibody Tagging

A Universal Approach to Targeted Molecular Imaging and Cell Homing in Cardiovascular Disease

H.T. Ta, S. Prabhu, E. Leitner, F. Jia, D. von Elverfeldt, Katherine E. Jackson, T. Heidt, A.K.N. Nair, H. Pearce, C. von zur Muhlen, X. Wang, K. Peter,* C.E. Hagemeyer*

Rationale: **Antibody-targeted delivery of imaging agents can enhance the sensitivity and accuracy of current imaging techniques. Similarly, homing of effector cells to disease sites increases the efficacy of regenerative cell therapy while reducing the number of cells required. Currently, targeting can be achieved via chemical conjugation to specific antibodies, which typically results in the loss of antibody functionality and in severe cell damage. An ideal conjugation technique should ensure retention of antigen-binding activity and functionality of the targeted biological component.**

Objective: **To develop a biochemically robust, highly reproducible, and site-specific coupling method using the *Staphylococcus aureus* sortase A enzyme for the conjugation of a single-chain antibody (scFv) to nanoparticles and cells for molecular imaging and cell homing in cardiovascular diseases. This scFv specifically binds to activated platelets, which play a pivotal role in thrombosis, atherosclerosis, and inflammation.**

Methods and Results: **The conjugation procedure involves chemical and enzyme-mediated coupling steps. The scFv was successfully conjugated to iron oxide particles (contrast agents for magnetic resonance imaging) and to model cells. Conjugation efficiency ranged between 50% and 70%, and bioactivity of the scFv after coupling was preserved. The targeting of scFv-coupled cells and nanoparticles to activated platelets was strong and specific as demonstrated in in vitro static adhesion assays, in a flow chamber system, in mouse intravital microscopy, and in in vivo magnetic resonance imaging of mouse carotid arteries.**

Conclusions: **This unique biotechnological approach provides a versatile and broadly applicable tool for procuring targeted regenerative cell therapy and targeted molecular imaging in cardiovascular and inflammatory diseases and beyond. (*Circ Res*. 2011;109:365-373.)**

Key Words: molecular imaging ■ platelets ■ thrombosis ■ antibodies ■ targeted molecular therapy ■ sortase A ■ cell therapy

Targeted delivery increases the efficacy of drugs and regenerative cell therapy, reduces the dose required, and consequently minimizes potential negative side effects. Similarly, targeted delivery of imaging agents can localize and retain contrast at disease sites, enhancing the sensitivity and accuracy of current imaging techniques. Targeting can be achieved via conjugation to antibodies that possess a number of functional groups, such as amine, thiol, and carboxylate groups suitable for chemical conjugation purposes.[1] Most antibody conjugation methods target endogenous amino acids, such as the amino group of lysine or the thiol group of cysteine[2]; however, these groups are commonly distributed throughout the antibody structure. If the conjugation involves critical residues essential for antigen binding, the functionality of antibodies, particularly small recombinant antibody fragments, will be impaired. Conjugation can also take place by use of the carbohydrate chains typically attached to the constant heavy chain domain within the crystallizable fragment region of the antibody[3]; however, this method is limited to glycosylated antibodies. Furthermore, conventional bioconjugation typically leads to multicomponent heterogenous mixtures that are incapable of complying with regulatory requirements. Overall, a single and covalent bond between an antibody and a

Original received December 3, 2010; resubmission received May 26, 2011; revised resubmission received June 7, 2011; accepted June 14, 2011. In May 2011, the average time from submission to first decision for all original research papers submitted to *Circulation Research* was 14.5 days.

From Atherothrombosis and Vascular Biology (H.T.T., S.P., E.L., F.J., K.E.J., A.K.N.N., H.P., X.W., K. Peter, C.E.H.), Baker IDI Heart and Diabetes Institute, Melbourne, Victoria, Australia; Departments of Medicine (S.P., X.W., K.P.), Clinical Haematology (A.K.N.N., C.E.H.), and Immunology (K.P., C.E.H.), Monash University, Melbourne, Victoria, Australia; Department of Medical Physics (D.v.E.), University Medical Center, Freiburg, Germany; and Department of Cardiology (T.H., C.v.z.M.), University Hospital, Freiburg, Germany.

*These authors were equally contributing senior authors.

Correspondence to Christoph E. Hagemeyer, PhD, Atherothrombosis and Vascular Biology, Baker IDI Heart and Diabetes Institute, PO Box 6492, St Kilda Rd Central, Victoria 8008, Australia. E-mail christoph.hagemeyer@bakeridi.edu.au

Circulation Research **is available at http://circres.ahajournals.org** **DOI: 10.1161/CIRCRESAHA.111.249375**

Non-standard Abbreviations and Acronyms	
CHO	Chinese hamster ovary
LIBS	ligand-induced binding sites
MPIO	microparticles of iron oxide
scFv	single-chain antibody

conjugation partner that preserves the functionality of both components is of critical importance and has a multitude of potential applications in the field of diagnostic and therapeutic antibody development.

Current coupling approaches for site-specific conjugation are based on the introduction of unique functional groups such as ketones and azides into proteins not present in natural amino acids. They can be incorporated into proteins by chemical modification of the N-terminus of the protein,[4] by unnatural amino acid mutagenesis,[5] or by the use of enzymes that transfer prosthetic groups to proteins.[6] However, these methods face practical limitations in terms of feasibility, scalability, and efficacy.[7]

In the present study, we demonstrate a new chemoenzymatic method to conjugate a single-chain antibody (scFv) to enhanced green fluorescent protein (eGFP), Chinese hamster ovarian (CHO) cells, human cord blood mononuclear cells, and microparticles of iron oxide (MPIOs) in a site-specific manner. This procedure uses *Staphylococcus aureus* enzyme sortase A, an enzyme that recognizes diverse substrates via an LPXTG motif, and conjugates this tag to a polyglycine nucleophile.[8] We engineered an LPETG-tagged scFv targeted to ligand-induced binding sites (LIBS) on glycoprotein (GP) IIb/IIIa (CD41/CD61) receptors, the most highly expressed molecules on the surface of activated platelets and critical players in atherosclerosis, thrombosis, and inflammation.[9,10] The conjugation method described in the present report comprises 2 stages: (1) the introduction of GGG peptides (as sortase nucleophiles) to the surface of magnetic particles and cells by a series of chemical reactions, and (2) the incubation of triglycine-tagged components with the sortase A enzyme and anti-LIBS scFv (Figure 1).

We demonstrate this novel use of sortase A for the selective labeling of imaging contrast particles and live cells with scFvs suitable for targeted molecular imaging and cell homing. This method is universally applicable and is particularly suitable for the antibody "tagging" of proteins, particles, or cells.

Methods

An expanded Methods section is available in the Online Data Supplement at http://circres.ahajournals.org.

Generation and Production of Proteins

The generation of the anti-LIBS scFv from a hybridoma cell line that expresses a monoclonal antibody against LIBS epitopes on GP IIb/IIIa has been described previously.[11] The LPETG motif was introduced to the C-terminal end of anti-LIBS scFv, and the scFv was subcloned into a pMT vector (Invitrogen, Carlsbad, CA) for expression in insect cells (Invitrogen). The GGG motif was introduced to the N-terminal end of the eGFP sequence by polymerase chain reaction, and GGG-eGFP was expressed in BL21-DE3 *Escherichia coli* (New England Biolabs, Ipswich, MA). The generation of the plasmid construct *Staphylococcus aureus* sortase[8] and the expression and production of soluble sortase A[12] were described previously.

Conjugation of Anti-LIBS to GGG-eGFP, Amine-Tagged Iron Oxide Particles, and Cells

The overall eGFP and particle-coupling procedures are summarized in Figures 1A and 1B, respectively. Anti-LIBS-LPETG scFv was coupled onto the cell surface by 2 methods. In the first

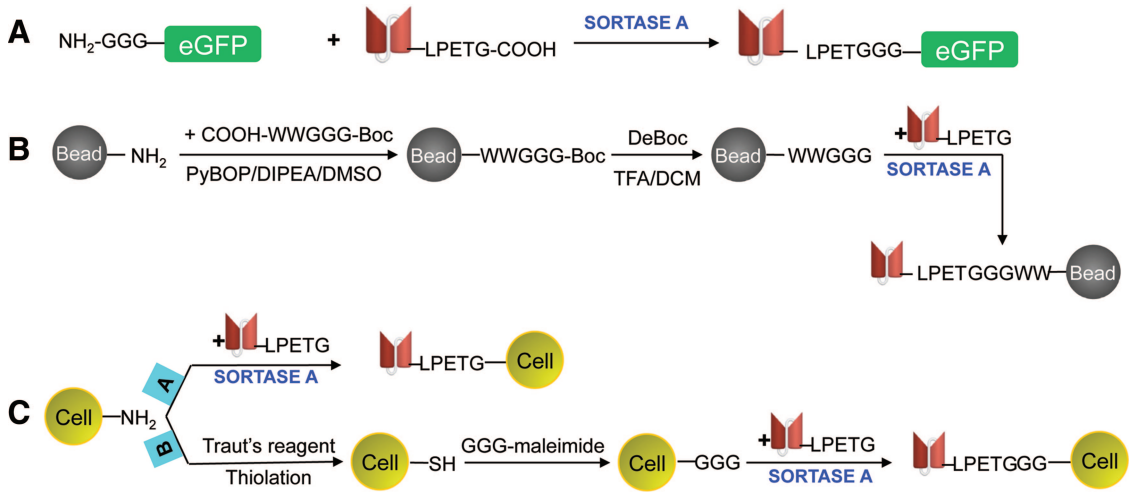

Figure 1. Image illustrating the coupling procedures of eGFP, MPIOs, and CHO cells with anti-LIBS-LPETG. A, eGFP: Sortase A catalyzed a condensation reaction between a C-terminal–LPETG tag on the GP IIb/IIIa–targeting single-chain antibody (anti-LIBS) and a triglycine (GGG) bridge on the eGFP protein. **B**, MPIO: tert-butyloxycarbonyl–protected GGGWW peptides were introduced onto amine particles via carboxyl activation. After deprotection, a sortase-mediated condensation reaction between anti-LIBS LPETG and GGG particles was performed. **C**, CHO cell: Protocol A comprised the sortase-catalyzed reaction between anti-LIBS LPETG and amine groups of the cell surface. Protocol B included the thiolation of cell membrane amine groups (sulfhydryl addition), the introduction of GGG maleimide on the cell surface via the reaction between the sulfhydryl (-SH) groups and the maleimide groups, and covalent coupling between anti-LIBS LPETG and GGG groups on the cell membrane via the sortase-mediated reaction.

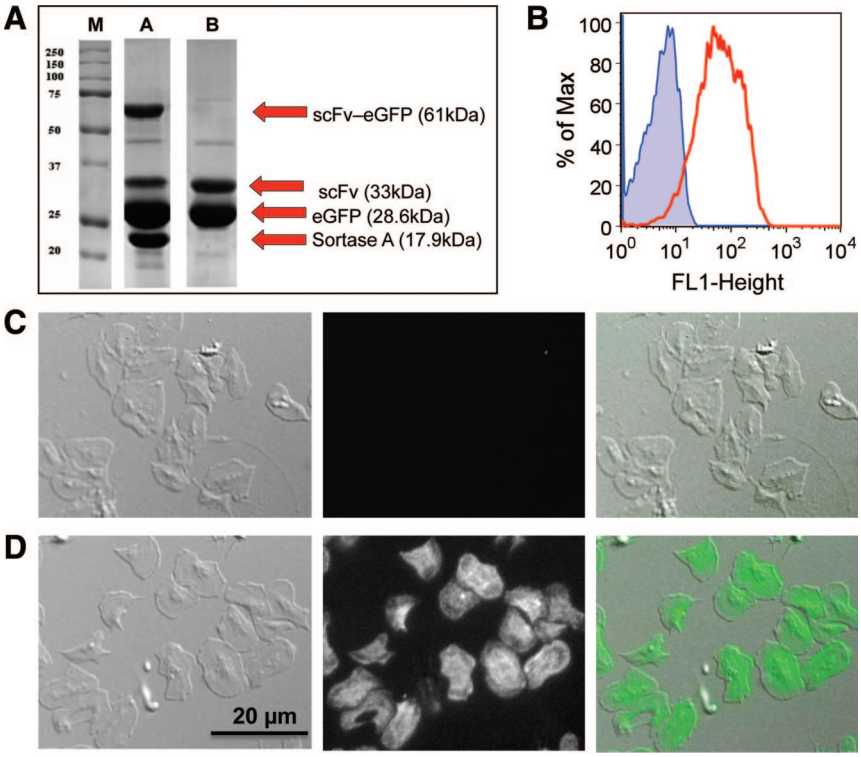

Figure 2. Conjugation of scFv to eGFP. **A**, Gel demonstrating the formation of coupled scFv-eGFP product. Gel showing a mixture of LPETG-tagged scFv and GGG eGFP both with (lane A) and without (lane B) sortase. A 61-kDa band representing coupled scFv-eGFP product is seen in lane A but is absent in lane B (negative control, without sortase). **B**, Flow cytometry histogram illustrating specific binding of scFv-eGFP to activated platelets (red) and nonbinding to nonactivated platelets (blue). Max indicates maximum. **C** and **D**, Bright field, fluorescence, and merged images demonstrate the retained functionality of coupled eGFP-scFv products (binding to fibrinogen-adhered activated platelets): control (**C**) and scFv-eGFP (**D**).

method, only 1 step was used. In the second method, 3 steps were used. The overall cell-coupling procedures are summarized in Figure 1C. The efficiency of the coupling procedure was analyzed by SDS-PAGE.

Flow Cytometry

Blood from healthy volunteers taking no medication was collected by venipuncture, anticoagulated with citric acid, and centrifuged to collect platelet-rich plasma. Diluted platelet-rich plasma was either activated by 20 μmol/L ADP (Sigma, St. Louis, MO) or nonactivated and incubated with different concentrations of the coupled anti-LIBS-eGFP products. Samples were fixed and analyzed by FACSCalibur (BD Biosciences, San Jose, CA).

Static Adhesion Assays

Glass coverslips were coated with either gel-filtered platelets or purified platelets and then incubated with predetermined numbers of either nontargeted or targeted products. Coverslips were then washed and fixed with CellFIX (BD Biosciences). Differential interference contrast/fluorescence images were taken at 600× or 200× magnification with an inverted microscope (IX81; Olympus, Tokyo, Japan) with a digital black-and-white camera (XM10; Olympus) and CellP 1692 (AnalySIS Image Processing; Olympus) software. Binding particles/cells were quantified with ImageJ (NIH, Bethesda, MD) software (n=6).

Flow Chamber Assays

Glass capillaries were coated with collagen-1 and then blocked with BSA (both, Sigma). Blood was taken from healthy donors, citrated, and perfused through the capillary for 5 minutes to allow the formation of thrombi. After washing, particles (Invitrogen) or cells (3×10^6 particles or cells per milliliter) were perfused through the capillary for 5 minutes at different shear rates ranging from 100 to 1500 s^{-1}. Movies/images were taken at 200× magnification with the above-described optics system. Thrombi were specifically stained with PAC-1-FITC or CD62P-PE (BD Biosciences). Binding particles or cells were quantified with ImageJ (NIH) software (n=3).

Intravital Studies

C57BL/6 wild-type mice (weight 15 to 17 g) were anesthetized by ketamine/xylazine (Bayer, Leverkusen, Germany). The injury of arteries/veins was induced by a microdrop of 10% $FeCl_3$ (Sigma). When the thrombus began to build up, predetermined amounts of particles or CHO cells were injected via a jugular vein cannula (n=3). Movies and images of the thrombus were taken before, during, and after injection at 200× magnification with the above-described optics system. Particles were seen by their TRITC autofluorescence, and CHO cells were visualized by CellTracker Green CMFDA dye (Invitrogen).

Magnetic Resonance Imaging Experiments and Histology

C57BL/6 wild-type mice were anesthetized, and carotid arterial wall–adherent thrombosis was induced with 6% ferrous chloride (Sigma). A total of 4×10^8 MPIOs (Invitrogen) was injected via tail vein. Magnetic resonance imaging (MRI) and histology procedures were conducted as described previously.[13]

Statistical Analysis

Results are presented as mean±SD. Data were analyzed for statistical significance with the 1-tailed paired *t* test. The data were checked for normal distribution by Kolmogorov-Smirnov normality test. Where normal distribution could not be detected, a nonparametric Mann Whitney 1-tailed test was applied. $P\leq0.05$ was considered significant.

Results

Characterization and Optimization of Sortase-Mediated Coupling With scFvs

First, eGFP was selected as a model substrate to establish optimal enzymatic reaction conditions for the coupling to anti-LIBS scFv, an scFv directed against LIBS on GP IIb/IIIa. Figure 2A demonstrates the formation of scFv-eGFP via sortase A enzyme coupling. Optimization of the

reaction conditions enabled maximization of the coupled product yield while making the most efficient use of substrate materials. These included variations in $CaCl_2$, substrate, and enzyme concentrations. Sortase A is a calcium-dependent transpeptidase that requires the presence of free calcium ions for its coupling activity; however, it was observed that in the presence of calcium, the scFv became insoluble in a dose-dependent manner, which caused it to precipitate and reduced its availability for coupling. Increasing concentrations of $CaCl_2$ formed progressively less coupled product, as evidenced by the diminishing 61-kDa band at higher concentrations of calcium (Online Figure I, A). At 0.5 mmol/L, we found no detectable evidence of precipitation and consequently a much higher amount of coupled product. A nearly proportional relationship between scFv concentration and coupled construct formation was also demonstrated (Online Figure I, B). Notably, there was little effect on the amount of coupled construct produced by increasing the concentration of the GGG-eGFP (Online Figure I, C). Online Figure I, D suggests that an increase in sortase concentration can improve the yield of the coupled product; however, this appeared to plateau beyond 5 to 10 μmol/L. Taken together, these results suggest that 0.5 mmol/L $CaCl_2$ and 10 μmol/L sortase are optimal parameters for the sortase-mediated reaction.

We demonstrated the retained functionality of the scFv after sortase-mediated coupling to the eGFP molecule in a flow cytometric analysis (Figure 2B). Figures 2C and 2D show the selective binding of the scFv-eGFP construct to activated platelets adhered to fibrinogen-coated glass coverslips. Activated platelets were stained with the coupled product and visualized by fluorescence microscopy. These results indicate the preserved specific targeting of the scFv after the conjugation process.

Conjugation of Anti-LIBS LPETG to Amine-Tagged Iron Oxide Microparticles and the Specific Binding of the Coupled Particles to Activated Platelets In Vitro

Next, we investigated the conjugation of anti-LIBS scFv to iron oxide particles using sortase and assessed the efficacy by gel electrophoresis. We found that anti-LIBS could be specifically conjugated onto particles at a yield of 0.21 ± 0.015 pg of anti-LIBS per particle ($n=3$; Online Figure II, Ac). Approximately 70% of the anti-LIBS amount in the reaction was successfully coupled to the particles. In the absence of sortase A, the nonspecific binding of scFv to particles was significantly lower than the specific binding in the presence of sortase A (Online Figure II, Ab). The results demonstrated the specific catalytic activity of sortase A in the condensation reaction between anti-LIBS LPETG and GGG particles.

In adhesion assays, anti-LIBS particles bound specifically to activated GP IIb/IIIa receptors on platelets. Online Figure II, B shows the significantly higher numbers of scFv-coupled particles binding on activated platelets compared with noncoupled particles (GGG particles). Increasing the number of particles incubated resulted in higher numbers of binding particles. Online Figure II, D illustrates the near absence of the binding of the nontargeting particles, whereas online Figure II, C demonstrates a large number of anti-LIBS particles binding to a single layer of activated platelets. Online Figure III represents the preserved functionality of anti-LIBS scFv and the preserved binding of targeted beads during storage at 4°C. The obtained data indicate the feasibility for storage of the targeted imaging agents for longer time periods.

Targeted Binding of Coupled Particles to Thrombi Under Flow Conditions

The adhesion of anti-LIBS–coupled particles to in vitro thrombi under shear stress was assessed in a flow chamber system (Figure 3). Shear stress was varied from 100 s^{-1} (venous flow) to 1500 s^{-1} (arterial flow). At both venous and arterial flows, the number of adherent coupled particles was significantly higher than that of noncoupled particles. Online Videos 1 and 2 show binding of particles at a shear stress of 500 s^{-1}.

To investigate the targeting ability of anti-LIBS particles in vivo, we used intravital imaging via differential interference contrast and fluorescence microscopy to directly visualize the binding of particles (orange autofluorescence) to thrombi in the observed artery. For each animal, 25×10^6 of either anti-LIBS or GGG particles was administered. The number of anti-LIBS–coupled particles adhering to the thrombi was significantly higher than that of the control GGG particles. Immediately after injection, anti-LIBS particles were found along the surface of the thrombus. As seen in Figure 4B and Online Video 4, a large number of targeted particles were attached to the thrombi, whereas only 1 control particle was found in Figure 4A and Online Video 3. We tested the effect of particles on thrombus formation by injecting the targeted constructs before the induction of thrombi and did not see an effect on thrombus formation. We also observed that in contrast to the postinjury injections, in which the constructs bound to the thrombus surface, in the preinjury injections, the contrast particles incorporated in the thrombus (Online Figures IV and V). To provide proof of concept for the suitability of our tagging approach for MRI, we performed in vivo MRI experiments using 1 μm of MPIOs because of their proven excellent magnetic resonance contrast properties as shown in previous reports from our group.[13–15] With these tagged particles, we could demonstrate excellent magnetic resonance signals in vivo (Online Figure VI). Histological analysis of the injured carotid artery demonstrated MPIOs that bound on the induced thrombus, which occupied approximately 20% of the vessel lumen (Online Figure VII).

Cell Anti-LIBS Conjugation and Functional Assessment in Static Adhesion Assay

The above procedure was adapted to the coupling of scFv to cells to assign unique and generally applicable targeting properties to cells. This approach is composed of 3 steps, described in protocol B in Figure 1C. Parameters in steps 1 and 2 were optimized by use of near-infrared DyLight

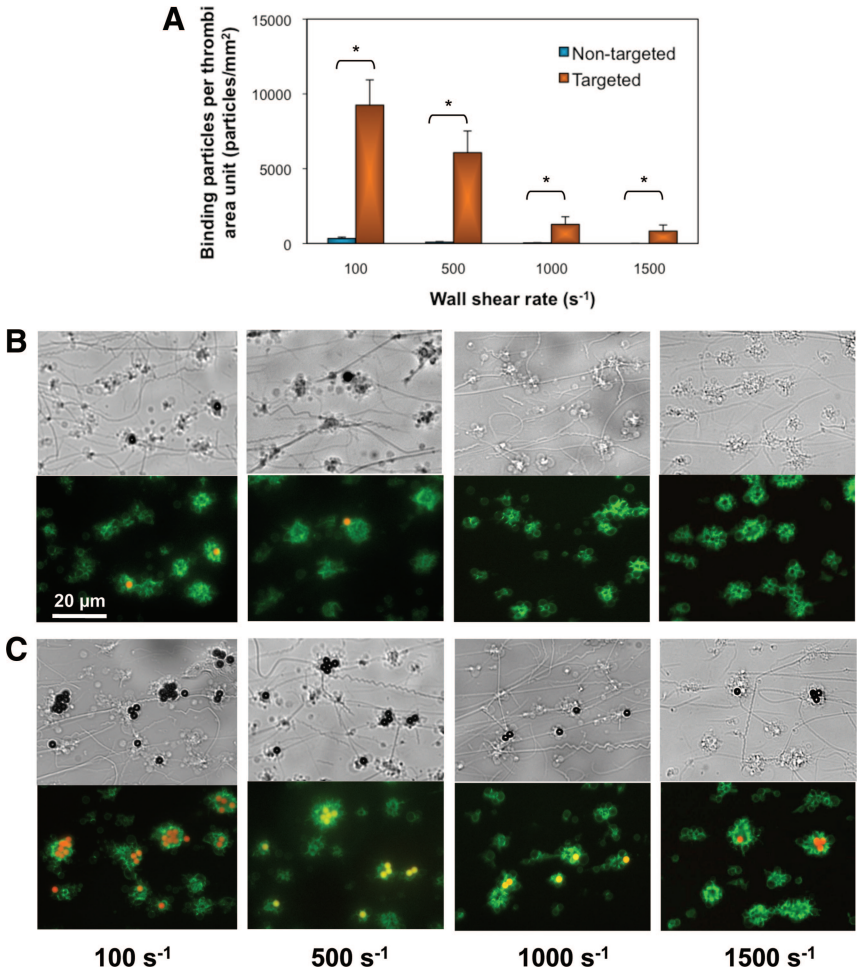

Figure 3. Specific binding of scFv-coupled particles to platelet aggregates in a flow chamber system. A, Number of particles binding to thrombus under different shear rates (*$P<0.05$; n=3 to 4; Mann-Whitney 1-tailed test) after 5 minutes of perfusion. **B**, Differential interference contrast (DIC) and fluorescence images show the lack of binding of the control particles (DIC images: black; fluorescence images: orange or yellow autofluorescence). Platelet aggregates (DIC: white or gray; fluorescence: green indicates platelet membrane) formed by aggregation of activated platelets on collagen-1 fibers were coated on the flow chamber surface. Platelet membranes were specifically stained with PAC-1-FITC directed toward GP IIb/IIIa receptors and appear as green fluorescence. **C**, DIC and fluorescence images show the strong binding of the scFv-coupled particles.

800 maleimide instead of NH_2-GGG-maleimide peptide, whereas optimal parameters in step 3 were determined by use of eGFP-LPETG instead of anti-LIBS LPETG. We used a reaction that contained cells without GGG tags, eGFP-LPETG, and sortase A as a negative control. Interestingly, we found that eGFP-LPETG was successfully coupled to CHO cells in the absence of the GGG groups (Online Figure VIII). The flow histograms of cells from this control reaction detected considerably more fluorescence than those incubated without sortase A. This finding suggested another cell-labeling method, which is described as protocol A in Figure 1C; however, its efficiency was significantly lower than that in protocol B, which comprised the full 3 steps (Online Figure VIII). It is possible that free amine groups on cell surface receptors function as a nucleophile for the enzyme, although the acyl-enzyme intermediate is less reactive toward an alkylamine than toward GGG or Gly_n. Parthasarathy et al[12] also reported the conjugation of eGFP-LPETG to amine-tagged particles and amine-terminated poly(ethylene) glycol by the sortase A enzyme. Overall, the successful labeling of eGFP on CHO cell surfaces provides proof of concept for the coupling of scFv onto cells.

Gel electrophoresis analysis of the reaction mixture (Online Figure IX, A) revealed that the average coupling efficiency was 10.08±3.15 pg (n=3) of anti-LIBS per CHO cell in protocol B, a 2-fold increase compared with that in protocol A. In static adhesion assays, the binding of the scFv-conjugated cells from both protocols was significantly stronger than the control (GGG) cells (Online Figure IX, B and C). The degree of binding increased with higher cell numbers in a dose-dependent manner. Notably, the binding efficiency of anti-LIBS–conjugated cells from protocol B was 5- to 7-fold higher than that produced by protocol A, which indicates the successful immobilization of a higher number of scFvs on the cell surface for targeting.

Targeting of Anti-LIBS Cells to Thrombi Under Shear Conditions

Anti-LIBS–coupled CHO cells from protocol B were investigated further in flow experiments under different shear rates. After targeted cells were perfused through a platelet-coated capillary at 100 s^{-1} for 5 minutes, approximately 400 cells/mm^2 platelet aggregates were immobilized (Figure 5; Online Video 5), whereas fewer than 10 nontargeted cells bound to a unit area (mm^2) of platelet aggregates (Figure 5; Online Video 6). At a shear rate of 250 s^{-1}, the number of binding cells decreased to 150 cells/mm^2 platelet aggregate, which indicates shear-dependent targeting efficacy. At 500 s^{-1}, the binding of MPIOs was reduced significantly; however, we still

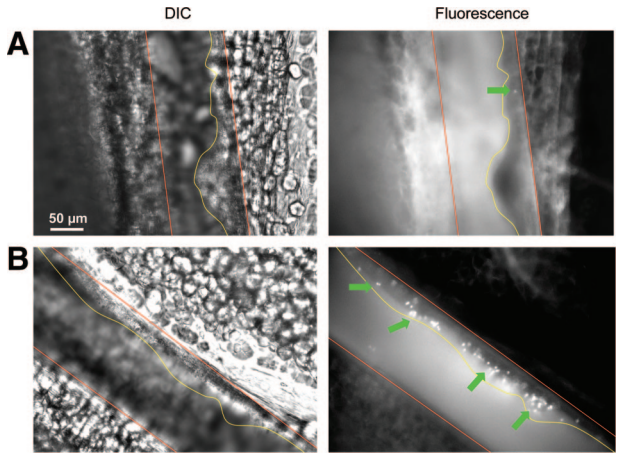

Figure 4. In vivo differential interference contrast (DIC) and fluorescence images demonstrating the targeting of scFv-coupled particles to platelet aggregates (thrombi) in a mesenteric artery (≈100 μm in diameter). Small particles (2.7 μm) were detected by fluorescence imaging but not by DIC. **A**, Almost no control (GGG) particles bound to the induced thrombus. **B**, Plenty of scFv-conjugated particles bound along the thrombus immediately after their injection. Thrombi are shown as yellow-outlined objects; arteries are red-outlined; and scFv-particles are round and white in fluorescence images. Some typical particles are indicated by green **arrows**.

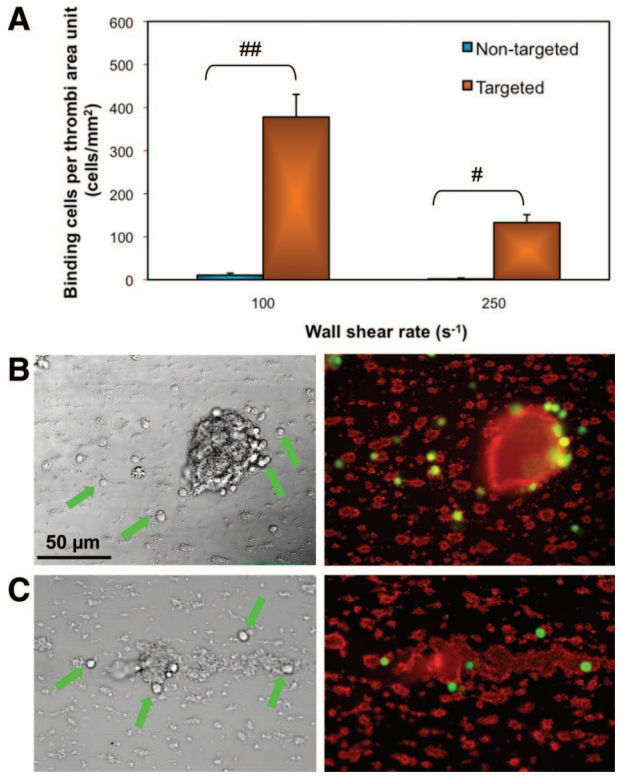

Figure 5. Targeting of scFv-coupled CHO cells to platelet aggregates under shear rates in a flow chamber system after 5 minutes. A, Number of nontargeted cells (GGG cells) and targeted cells (scFv cells) binding to thrombus under different shear rates (#$P<0.05$, ##$P<0.01$; n=3 to 5; Mann-Whitney 1-tailed test) after 5 minutes of perfusion. **B** and **C**, Differential interference contrast and fluorescence images show the binding of targeted cells (differential interference contrast images: round gray or white, indicated by green **arrows**; fluorescence images: green or yellow) on platelet aggregates (differential interference contrast image: white or gray; fluorescence image: red indicates platelet membrane) under shear rates of 100 and 250 s^{-1}, respectively. CHO cells were stained with CellTracker. Platelet aggregates formed by the aggregation of activated platelets on collagen-1 fibers were immobilized on the chamber surface and specifically stained with phycoerythrin-labeled anti-CD62P.

observed some adherent cells, which bound primarily to larger thrombi (data not shown). To demonstrate the suitability of cell tagging for native human cells, the scFv was also coupled to mononuclear cells isolated from human cord blood using the same conjugation protocol. Online Figure X shows the specific binding of mononuclear cells to thrombi at a shear rate of 250 s^{-1}. Finally, intravital microscopy was used to evaluate the targeting of anti-LIBS–coupled cells to activated platelets in mouse mesenteric veins. After the administration of 10×10^6 CHO cells, we noted a significantly higher number of anti-LIBS–conjugated cells binding on the venous thrombi compared with the control (GGG-tagged) cells (Figure 6; Online Videos 7 and 8), which indicates successful in vivo cell targeting with this novel approach.

Discussion

We report a chemoenzymatic method for conjugation of recombinant antibody fragments as targeting ligands to contrast agents and cells, with potential applicability to a broad range of areas including molecular imaging, regenerative cell therapy, and drug delivery. This method combines chemical reactions with a sortase-mediated enzymatic coupling. With eGFP used as a model substrate, optimal enzymatic reaction conditions specific for scFv were established. The scFv was conjugated to MPIOs (contrast agents for MRI) and to model cells (CHO), as well as to human mononuclear cells, with a high efficiency (up to 72%) and preserved scFv bioactivity. The targeting of scFv-coupled contrast particles and cells to activated platelets was demonstrated in vitro with adhesion assays under static and flow conditions. We also successfully demonstrated the retained targeting capability of our conjugation products in vivo. Immediately after injection, we observed strong adhesion of anti-LIBS–conjugated contrast agents at sites of induced thrombi in mesenteric arteries. Furthermore, the suitability of particle tagging for molecular imaging was demonstrated in MRI of carotid artery thrombosis in mice. Finally, sortase-coupled cells could be targeted successfully toward activated platelets on injured endothelium. Overall, this specific targeting approach describes a unique and broadly usable strategy for molecular imaging and cell therapy in thrombotic, atherosclerotic, and inflammatory diseases.

Since the discovery and the isolation of sortase A from *S aureus*,[8] this enzyme has been used primarily as an engineering tool, eg, to immobilize proteins to solid surfaces such as polystyrene beads,[12] biosensor chips,[16] and microspheres[17] or to synthesize neoglycoconjugates.[18] In addition, recent protein/peptide-protein/peptide oligomerization[12] and labeling of proteins on cells[19] have demonstrated its applicability toward biological use. The present work is the first report of sortase-mediated ligation

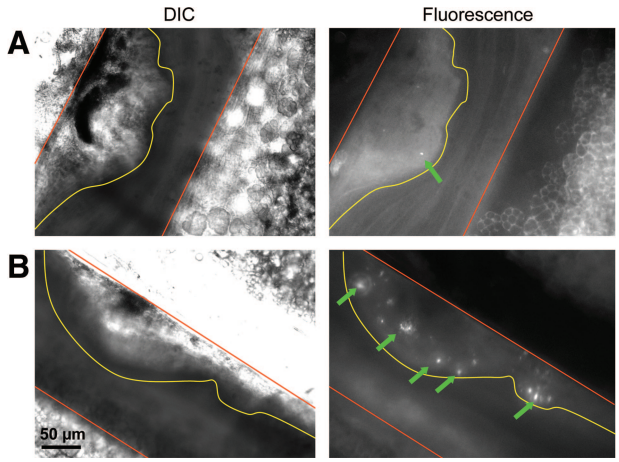

Figure 6. In vivo demonstration of the targeted binding of scFv-coupled cells to thrombi in mouse mesenteric veins (≈150 to 180 μm in diameter). Fluorescence images visualizing stained cells. **A**, Few GGG-tagged cells adhered on the induced thrombus, whereas in panel **B**, many scFv-conjugated cells were targeted to the thrombus soon after their administration. Thrombi are seen as yellow-outlined objects; arteries are red-outlined; and scFv-cells are round and white in fluorescence images. Some typical cells are indicated by green **arrows**. Cells appear as different sizes because of their location on different focus levels.

of antibodies, or indeed coupling of any targeting protein, and the first demonstration of the in vivo use of the sortase technology. The 2 required short motifs (LPETG and GGG) can be incorporated into substrates of interest either by chemical synthesis or by genetic engineering. We introduced the LPETG motif to anti-LIBS at the C-terminus by polymerase chain reaction cloning while preserving the functionality of the scFv. In addition to their ease of production and limited immunogenicity, scFvs have a structure particularly suitable for sortase-mediated coupling.[20] The C-terminal end is not within the targeting regions of the scFv, thus minimizing the likelihood of compromising the antigen-binding region.

Previously, we have used a noncovalent coupling method between the C-terminal His-tag of the scFv and ion metal groups on MPIOs for molecular MRI.[13–15] Despite its speed and simplicity, this method is not biocompatible and therefore not suitable for human use. We addressed the challenge of efficient, covalent, and biocompatible conjugation between MPIOs and the anti-LIBS scFv as part of our endeavors to translate the anti-LIBS targeting antibody into a clinical diagnostic imaging product. The robust, specific, and gentle sortase-mediated chemoenzymatic condensation provides a useful alternative to chemical ligation, thereby fulfilling an essential requirement for targeted imaging. Alternative related bioconjugation methods such as native chemical ligation,[21] intein-based ligation,[22] and very few other enzyme-based approaches have been reported.[23] However, these reported methods have common limitations, including the difficulty of synthesizing peptide thioesters, large tags that can lead to expression problems,[24] and an inefficient stepwise ligation procedure. The present MRI data demonstrate that the high signal strength of MPIOs is ideally suited for in vivo MRI in small animals and could be rapidly translated to a clinical setting with biocompatible sortase-mediated bioconjugation. The described method can also be adapted to develop novel targeted radioisotope nanoparticles for molecular positron emission tomography, targeted iodine/gold nanoparticles for computed tomography, and targeted gadolinium nanoparticles for MRI. Targeted positron emission tomography/computed tomography imaging might minimize off-target effects, high background signals, and false-positive results. Targeted gadolinium nanoparticles would reduce side effects associated with gadolinium nephrotoxicity caused by the targeting approach and thereby lower the injected dose of gadolinium.

The present work is also directly relevant to regenerative stem cell therapy. Despite some promising progress, the full potential of this therapy has not yet been realized. A significant limiting factor is the low grafting efficiency of cells to the target tissue.[25] As demonstrated by the successful targeting of model CHO cells to platelets that adhered to injured endothelium, the described chemoenzymatic approach can specifically direct these cells to the site of disease. Thus, a strong enrichment of desired cells can be achieved. The potential application of this approach for stem cell therapy was also strengthened by the successful binding of mononuclear cells to activated platelets under shear stress in a flow chamber setting.

Our anti-LIBS scFv has a high and specific binding capability to activated GP IIb/IIIa, as demonstrated by the binding of MPIOs in mouse mesenteric and carotid arteries in the present study and by previous reports from our group.[13–15,26] Despite providing excellent targeting of smaller particles under arterial shear stress, targeting of CHO cells appears to be restricted to lower shear rates. This can be explained by the fact that CHO cells with a diameter of 10 to 15 μm (compared with 1 to 2.7 μm for MPIOs) will be subject to higher hemodynamic drag forces than smaller particles. However, leukocyte recruitment and stem cell homing are described as being localized to venules and thus (patho)physiologically take place under low shear conditions.[27,28] Inflammation (eg, caused by cerebral or myocardial ischemia/reperfusion) results in leukocyte recruitment and stem cell homing at the sites of venules.[29,30] In addition, in bone marrow, the recruitment site of hematopoietic cells has been found to be the venules, which exhibit a strong expression of adhesion molecules such as vascular cell adhesion molecule-1 and selectins.[31] Therefore, the present findings with antibody-targeted cells are in accordance with the (patho)physiology seen in stem cell homing or leukocyte recruitment with regard to the shear at which these phenomena occur.

Finally, the described method for tagging particles with antibodies is also relevant therapeutically in its application toward targeted drug-delivery vehicles. Nontargeted delivery of therapeutics often requires a high drug load and might cause off-target effects compared with targeted drug delivery. This has been demonstrated for the treatment of several diseases, including cancer[32] and cardiovascular

disease.[33] Despite the development of a large number of preclinical delivery systems, very few new technologies or materials have entered clinical trials. One hurdle is that regulatory approval requires well-defined products for clinical use. The first use of a targeted nanoparticle in humans was only recently reported with a phase I clinical trial of a delivery system for small interfering RNA to patients with solid cancers.[34] An efficient bioconjugation method such as sortase-mediated antibody tagging that retains functionality and avoids multicomponent mixtures has the potential to overcome a significant hurdle for a faster and broader translation of targeted drug delivery from bench to bedside.

In conclusion, the present data demonstrate the successful and specific chemoenzymatic conjugation of a recombinant antibody fragment to a reporter protein, contrast agents, and cells with sortase A. This method not only provides an efficient conjugation approach but importantly retains the functionality of the targeting antibody component and avoids heterogeneous multilabeled mixtures. The utility of this approach is potentially very broad, with the conjugation of any triglycine-containing substrate/cell/particle to any LPETG-containing substrate/cell/particle. Both LPETG and GGG are unique, thereby providing highly specific coupling. More specifically, this work establishes sortase-mediated bioconjugation as a potentially universal and versatile technique for antibody-targeted molecular imaging and regenerative cell therapy.

Sources of Funding

This work was funded by National Health and Medical Research Council (NHMRC) project and development grants 472665 and 472667; the International Science Linkages program (Grant CG130101) from the Department of Innovation, Industry, Science and Research; National Heart Foundation Grant-in-Aid G09M4345 (H.P., C.E.H.); the German Research Foundation (Mu 2727/3-1); National Heart Foundation Postdoctoral Fellowship PF 09M 4688 (H.T.T.); Australian Research Council Future Fellowship FT0992210 (K.P.); and NHMRC Career Development Award 472668 (C.E.H.). The study was supported in part by the Victorian Government's Operational Infrastructure Support Program.

Disclosures

None.

References

1. Hermanson GT. Antibody modification and conjugation. *Bioconjugate Techniques*. Oxford, United Kingdom: Academic Press; 2008: 783–823.
2. Junutula JR, Raab H, Clark S, Bhakta S, Leipold DD, Weir S, Chen Y, Simpson M, Tsai SP, Dennis MS, Lu Y, Meng YG, Ng C, Yang J, Lee CC, Duenas E, Gorrell J, Katta V, Kim A, McDorman K, Flagella K, Venook R, Ross S, Spencer SD, Wong WL, Lowman HB, Vandlen R, Sliwkowski MX, Scheller RH, Polakis P, Mallet W. Site-specific conjugation of a cytotoxic drug to an antibody improves the therapeutic index. *Nat Biotechnol*. 2008;26:925–932.
3. Kaneko Y, Nimmerjahn F. Anti-inflammatory activity of immunoglobulin G resulting from Fc sialylation. *Science*. 2006;313:670–673.
4. Gilmore JM, Scheck RA, Esser-Kahn AP, Joshi NS, Francis MB. N-terminal protein modification through a biomimetic transamination reaction. *Angew Chem Int Ed*. 2006;45:5307–5311.
5. Wang L, Schultz PG. Expanding the genetic code. *Angew Chem Int Ed*. 2004;44:34–66.
6. Chen I, Howarth M, Lin W, Ting AY. Site-specific labeling of cell surface proteins with biophysical probes using biotin ligase. *Nat Methods*. 2005;2:99–104.
7. Wu P, Shui W, Carlson BL, Hu N, Rabuka D, Lee J, Bertozzi CR. Site-specific chemical modification of recombinant proteins produced in mammalian cells by using the genetically encoded aldehyde tag. *Proc Natl Acad Sci U S A*. 2009;106:3000–3005.
8. Ton-That H, Liu G, Mazmanian SK, Faull KF, Schneewind O. Purification and characterization of sortase, the transpeptidase that cleaves surface proteins of Staphylococcus aureus at the LPXTG motif. *Proc Natl Acad Sci U S A*. 1999;96:12424–12429.
9. Gawaz M, Langer H, May AE. Platelets in inflammation and atherogenesis. *J Clin Invest*. 2005;115:3378–3384.
10. von Hundelshausen P, Weber C. Platelets as immune cells: bridging inflammation and cardiovascular disease. *Circ Res*. 2007;100:27–40.
11. Schwarz M, Katagiri Y, Kotani M, Bassler N, Loeffler C, Bode C, Peter K. Reversibility and persistence of GPIIb/IIIa blocker-induced conformational change of GPIIb/IIIa (cd41/cd61). *J Pharmacol Exp Ther*. 2004; 308:1002–1011.
12. Parthasarathy R, Subramanian S, Boder ET. Sortase A as a novel molecular "stapler" for sequence-specific protein conjugation. *Bioconjug Chem*. 2007;18:469–476.
13. von zur Muhlen C, von Elverfeldt D, Moeller JA, Choudhury RP, Paul D, Hagemeyer CE, Olschewski M, Becker A, Neudorfer I, Bassler N, Schwarz M, Bode C, Peter K. Magnetic resonance imaging contrast agent targeted toward activated platelets allows in vivo detection of thrombosis and monitoring of thrombolysis. *Circulation*. 2008;118: 258–267.
14. von zur Muhlen C, Peter K, Ali ZA, Schneider JE, McAteer MA, Neubauer S, Channon KM, Bode C, Choudhury RP. Visualization of activated platelets by targeted magnetic resonance imaging utilizing conformation-specific antibodies against glycoprotein IIb/IIIa. *J Vasc Res*. 2009;46:6–14.
15. von Zur Muhlen C, von Elverfeldt D, Choudhury RP, Ender J, Ahrens I, Schwarz M, Hennig J, Bode C, Peter K. Functionalized magnetic resonance contrast agent selectively binds to glycoprotein IIb/IIIa on activated human platelets under flow conditions and is detectable at clinically relevant field strengths. *Mol Imaging*. 2008;7:59–67.
16. Clow F, Fraser JD, Proft T. Immobilization of proteins to biacore sensor chips using staphylococcus aureus sortase A. *Biotechnol Lett*. 2008;30: 1603–1607.
17. Wu S, Proft T. The use of sortase-mediated ligation for the immobilisation of bacterial adhesins onto fluorescence-labelled microspheres: a novel approach to analyse bacterial adhesion to host cells. *Biotechnol Lett*. 2010;32:1713–1718.
18. Samantaray S, Marathe U, Dasgupta S, Nandicoori VK, Roy RP. Peptide-sugar ligation catalyzed by transpeptidase sortase: a facile approach to neoglycoconjugate synthesis. *J Am Chem Soc*. 2008;130: 2132–2133.
19. Tanaka T, Yamamoto T, Tsukiji S, Nagamune T. Site-specific protein modification on living cells catalyzed by sortase. *Chembiochem*. 2008;9: 802–807.
20. Hagemeyer CE, Schwarz M, Peter K. Single-chain antibodies as new antithrombotic drugs. *Semin Thromb Hemost*. 2007;33:185–195.
21. Tam JP, Xu J, Eom KD. Methods and strategies of peptide ligation. *Biopolymers*. 2001;60:194–205.
22. Iakovenko A, Rostkova E, Merzlyak E, Hillebrand AM, Thoma NH, Goody RS, Alexandrov K. Semi-synthetic Rab proteins as tools for studying intermolecular interactions. *FEBS Lett*. 2000;468:155–158.
23. Rall K, Bordusa F. Substrate mimetics-specific peptide ligases: studies on the synthetic utility of a zymogen and zymogen-like enzymes. *J Org Chem*. 2002;67:9103–9106.
24. Nyanguile O, Dancik C, Blakemore J, Mulgrew K, Kaleko M, Stevenson SC. Synthesis of adenoviral targeting molecules by intein-mediated protein ligation. *Gene Ther*. 2003;10:1362–1369.
25. Chien KR. Regenerative medicine and human models of human disease. *Nature*. 2008;453:302–305.
26. Stoll P, Bassler N, Hagemeyer CE, Eisenhardt SU, Chen YC, Schmidt R, Schwarz M, Ahrens I, Katagiri Y, Pannen B, Bode C, Peter K. Targeting ligand-induced binding sites on GPIIb/IIIa via single-chain antibody allows effective anticoagulation without bleeding time prolongation. *Arterioscler Thromb Vasc Biol*. 2007;27:1206–1212.

27. Ritter LS, Orozco JA, Coull BM, McDonagh PF. Leukocyte accumulation and hemodynamic changes in the cerebral microcirculation during early reperfusion after stroke. *Stroke*. 2000;31:1153–1161.
28. Ritter LS, McDonagh PF. Low-flow reperfusion after myocardial ischemia enhances leukocyte accumulation in coronary microcirculation. *Am J Physiol Heart Circ Physiol*. 1997;273:H1154–H1165.
29. Ley K, Gaehtgens P. Endothelial, not hemodynamic, differences are responsible for preferential leukocyte rolling in rat mesenteric venules. *Circ Res*. 1991;69:1034–1041.
30. Yilmaz G, Vital S, Yilmaz CE, Stokes KY, Alexander JS, Granger DN. Selectin-mediated recruitment of bone marrow stromal cells in the postischemic cerebral microvasculature. *Stroke*. 2011;42:806–811.
31. Mazo IB, von Andrian UH. Adhesion and homing of blood-borne cells in bone marrow microvessels. *J Leukoc Biol*. 1999;66:25–32.
32. Brannon-Peppas L, Blanchette JO. Nanoparticle and targeted systems for cancer therapy. *Adv Drug Deliv Rev*. 2010;56:1649–1659.
33. Hallow DM, Mahajan AD, Prausnitz MR. Ultrasonically targeted delivery into endothelial and smooth muscle cells in ex vivo arteries. *J Control Release*. 2007;118:285–293.
34. Davis ME, Zuckerman JE, Choi CHJ, Seligson D, Tolcher A, Alabi CA, Yen Y, Heidel JD, Ribas A. Evidence of RNAi in humans from systemically administered siRNA via targeted nanoparticles. *Nature*. 2010;464:1067–1070.

Novelty and Significance

What Is Known?

- Targeted delivery can be achieved via the use of specific binding ligands, such as antibodies.
- Currently, binding ligands are conjugated primarily to therapeutic/imaging agents via chemical methods, which are not site specific and typically result in impaired ligand binding (eg, reduced antibody affinity), low product yields, and multicomponent mixtures.
- Some site-specific conjugation approaches have been reported, but they have practical limitations in terms of feasibility, scalability, and efficacy.

What New Information Does This Article Contribute?

- The article reports on a versatile and universally applicable site-specific conjugation method for targeted regenerative cell therapy and targeted molecular imaging in cardiovascular and inflammatory diseases.

We have developed a new, robust, and highly reproducible chemoenzymatic approach to obtain site-specific conjugation that preserves functionality of the binding ligands. With this method, an activation-specific antiplatelet single-chain antibody was successfully conjugated to a model protein, a magnetic resonance imaging agent, and 2 model cells, with high efficiency and good yield. The antibody-coupled products were targeted to activated platelets in both in vitro and in vivo settings in a specific and efficient manner. Our work is the first report of sortase-mediated ligation of antibodies, or indeed coupling of any targeting protein, and the first demonstration of in vivo use of the sortase technology. The method we have developed provides an efficient conjugation approach that retains the functionality of the targeting antibody component and avoids heterogeneous multilabeled mixtures. This unique biotechnological approach can be generalized to conjugate any antibody or other binding ligands to any triglycine containing substrates for targeting purposes.

SUPPLEMENTAL MATERIAL

DETAILED METHODS

Uniform and super-paramagnetic particles (2.7 μm) with amine groups on the surface were purchased from Dynal Biotech (USA). BocHN-GGGWW-OH peptide (734 Da) was obtained from GL Biochem (Shanghai, China) Ltd. NIR Dylight 800 maleimide was from Pierce Biotechnology (USA). Collagen-1 and SKF solution (for collagen dilution) were from Nycomed (Austria). PAC-1-FITC and CD62P-PE were purchased from BD Biosciences. Bovine serum albumin (BSA) and other chemical materials were obtained from Sigma-Aldrich (Australia). All cell culture reagents were obtained from GIBCO/Invitrogen (Australia) unless otherwise noted. Chinese Hamster Ovarian (CHO) cell line attained from the American Type Culture Collection (ATCC) was cultured in Dulbecco's modified Eagle's medium (DMEM) supplemented with 10% fetal bovine serum (FBS), 1% nonessential amino acids (NEAA) and 1% penicillin/streptomycin (P/S, Sigma) in a humidified 5% CO_2 atmosphere. A seeding cell population of exponentially-growing cells greater than 95% viability was used for all assays. C57BL/6 wild-type mice weighing less than 18 g obtained from Alfred Medical Research and Education Precinct Animal Services – AMREP AS Pty Ltd were used for all intravital microscopy experiments. All experiments involving animals were approved by the Alfred Medical Research and Education Precinct Animal Ethics Committee.

Generation of the single-chain antibody anti-LIBS with LPETG motif at the C-terminus

The generation of the anti-LIBS scFv from a hybridoma cell line expressing a monoclonal antibody against LIBS epitopes on GPIIb/IIIa has been described previously[1, 2]. To express anti-LIBS in insect cells, the scFv was cleaved at NcoI and NotI restriction sites and sub-cloned into a pMT vector system (Invitrogen, USA). To clone LPETG motif into pMT vector for generating the anti-LIBS-LPETG, we designed two complementary primers containing the LPETG sequence flanked by 5' NotI and 3' ApaI as following: sense strand: 5'-GCGGCCGCTCTGCCGGAAACCGGCGGCGGGCCCA-3', antisense strand: 5'-GGGCCCGCCGCCGGTTTCCGGCAGAGCGGCCGCA-3' (LPETG sequence underlined). Primers were also designed with A overhangs for sub-cloning into pGEM-T Easy vector (Invitrogen, USA). The primers were annealed to a double strand product, ligated into the pGEM-T Easy vector and transformed into DH5α *E.Coli* cells (Invitrogen, USA) for amplification of the vectors. pGEM-T Easy-LPETG was then digested with EcoRI and then with NotI and ApI. Subsequently, the amplified LPETG strands were cloned into pMT-anti-LIBS at NotI and ApaI restriction sites. The resulting plasmid constructs were then transformed into TG1 *E.Coli* cells (Invitrogen, USA). The transformed cells were grown in LB media containing 100 μg/ml ampicillin and 100 mmol/L glucose at 37˚C and the plasmids were purified using Plasmid Maxi Kit (Qiagen, Australia).

Expression and purification of scFv constructs in *Drosophila S2*

Drosophila S2 cells (Invitrogen, USA) were transfected with pMT-anti-LIBS-LPETG using a method described by Han et al[3]. Briefly, cells were diluted to 1×10^6 cells/ml and mixed with 80 ng/ml anti-LIBS-LPETG DNA preincubated with 250 ng/ml dimethyldioctadecylammonium bromide for 30 min. The cells were then cultured in Express Five SFM medium containing 18 mmol/L L-glutamine and 1% penicillin/streptomycin at 28°C in ventilated polycarbonate Erlenmeyer flasks (Corning, Acton, MA, USA) under constant rotation (100 rpm, Bench top Orbital Shaker Incubator, Ratek Instruments, Australia). After two days, protein production was induced by 500 μmol/L $CuSO_4$. Six days later, the cell supernatant was collected by centrifugation at 15,000 g for 15 min. The cell supernatant was applied to a chelating Sepharose fast flow column (20 ml bed volume, 5 ml/min flow rate, GE Healthcare, Uppsala, Sweden). The column was washed to baseline with PBS, 0.5 mol/L NaCl and 10 mmol/L imidazole in 50 mM Tris, pH 8.0 to remove non-specifically bound proteins. Elution was carried out with 250 mmol/L imidazole in 50 mmol/L Tris, pH 8.0. Fractions of 50 ml were collected. Fractions containing significant amounts of product were pooled and dialyzed

against PBS. A second purification was done with a nickel-based metal affinity chromatography column, Ni-NTA column (Invitrogen), according to the manufacturer's instruction manual. Fractions of 2 ml were collected and dialysed against PBS.

Generation, expression and production of GGG-eGFP

The following primers were designed to introduce the NdeI and XhoI restriction sites and GGG Sortase ligand into pEGFP-C1 vector (Clontech, USA): sense strand 5'-CATATG**GGAGGCGGCGGTTCA**ATGGTGAGCAAGGGCGAG-3', antisense strand 5'-CTCGAGCTTGTACAGCTCGTCCATG-3' (GGGWW in bold; NdeI and XhoI underlined, respectively). The amplification of GGG-eGFP sequence was performed by PCR using these primers. The PCR products were then cloned into a pET-20b(+) vector system at the NdeI and XhoI restriction sites. Amplification of the plasmids was done using XL1-B *E.Coli* cells (Invitrogen, USA) and the plasmid purification was performed using a Plasmid Mini-Prep Kit (Qiagen, Australia). GGG-eGFP was expressed in BL21-DE3 *E.Coli* (Invitrogen, USA). The cells were cultured in LB media containing 100 µg/ml ampicillin until the OD_{600} of 0.8 was reached. GGG-eGFP production was induced with 1 mmol/L of isopropyl β-D-1-thiogalactopyranoside (IPTG) for 4 hours at 37˚C. Bacteria were then isolated by centrifugation at 4000 rpm for 10 min. Proteins were purified using Ni-NTA column (Invitrogen), according to the manufacturer's protocol. Fractions of 2 ml were collected and dialysed against PBS.

Expression and production of Sortase A enzyme

S. aureus strain NCTC8325 was kindly provided by Dr. Howden (Microbiology Department, The University of Melbourne, Australia). The generation of the plasmid constructing *S.aureus* Sortase A was described by Ton-That et al[4]. Briefly, the following primers were used to PCR amplify the Sortase A sequence from the chromosome of *S. aureus:*

5'-AAAGGATCCAAACCACATATCGATAATTATC-3'and
5'-AAGGATCCTTATTTGACTTCTGTAGCTACAA-3'.

The DNA fragment was then cloned into a pQE30 vector system (Qiagen) at *Bam*HI restriction sites. The vector constructs were transformed into XL-1 *E. coli* (Invitrogen, Australia) and selected on Luria agar with ampicillin (100 µg/ml).

The expression and production of soluble Sortase A were described previously by Parthasarathy et al[5]. Briefly, the enzymes were expressed in BL21-DE3 *E. Coli* (Invitrogen, USA). Cultures were allowed to reach an OD_{600} of 0.7 and 1 mmol/L IPTG was added to induce the protein production for 3 hours at 37˚C. Proteins were purified using Ni-NTA column (Invitrogen), according to the manufacturer's protocol. Fractions of 2 ml were collected and dialysed against PBS.

Conjugation of anti-LIBS to GGG-EGFP and purification of the coupled products

1 ml reaction volume containing 20 µmol/L GGG-eGFP, 20 µmol/L anti-LIBS-LPETG, 10 µmol/L Sortase A, and 0.5 mmol/L $CaCl_2$ in Tris reaction buffer (50 mmol/L Tris, 150 mmol/L sodium chloride, pH 8) was incubated at 37˚C and 900 rpm for 3 hours in dark. The efficiency of the coupling procedure was analysed by SDS-PAGE. The resulted mixture was concentrated by centrifuging in a 10,000 kDa cut-off MWCO spin tube (Millipore, USA) for 6 min at 12,000 g. The coupled products were purified by size exclusion chromatography using a 120-ml HiPrep™ Sephacryl S-200 high resolution gel filtration column (GE Healthcare Lifesciences, Australia) configured to a Pharmacia Fast Protein Liquid Chromatography (FPLC) system (GE Healthcare Bio-Science, Australia). Briefly, the column was equilibrated with PBS without calcium and magnesium at 1 ml/min for 2 hours. Reaction mixture was added to the column at 0.5 ml/min, followed by continuous washing of the column at a rate of 0.5 ml/min with PBS without calcium and magnesium. Once a measurable increase in absorbance was detected (approximately 60 min), a recording of the elution profile was commenced and the eluate collected in 500-µl fractions, until absorbance returned to baseline levels. Fractions were analysed by SDS-PAGE to determine those containing predominately coupled product (based on the presence of a single 61 kDa band on SDS). The

concentration of each fraction was then determined using a BCA protein assay (Pierce, Australia). Fractions with the highest concentrations were pooled and stored at -80°C.

Conjugation of anti-LIBS-LPETG to 2.7µm amine-tagged iron-oxide particles

2 x 10^8 particles were washed once with water and once with dimethyl sulfoxide (DMSO). Particles were resuspended in 200 µl of DMSO and BocHN-GGGWW-OH peptide was added to a final concentration of 3.8 mmol/L (600 µg). Benzotriazol-1-yl-oxytripyrrolidino-phosphonium hexafluorophosphate (PyBOP - 1 equivalent, 400 µg, 3.8 mmol/L) and N,N-Diisopropylethylamine (DIPEA - 2 equivalent, 200 µg, 7.6 mmol/L) was dissolved in DMSO and added to the resulting solution. The mixture was incubated with shaking for 2 hours at room temperature. After being washed three times with deionized water, the particles were resuspended in 60 µl of 50% trifluoroacetic (TFA) in dichloromethane (DCM) and incubated for 30 min with shaking at room temperature to de-protect the amine groups of the conjugated peptide (de-Boc). After washings, the particles were incubated with 10% triethanolamine (TEA) in DCM at room temperature for 20 min. Particles were then washed twice with water and twice with Sortase coupling buffer (50 mmol/L Tris, 150 mmol/L NaCl, pH 8.0). 2 x 10^8 particles were resuspended in 200 µl of coupling buffer. Anti-LIBS-LPETG, Sortase A enzyme and $CaCl_2$ were added to the final concentration of 10 µmol/L, 10 µmol/L and 0.5 mmol/L, respectively. The reaction mixture was incubated at 37˚C for 3 hours with shaking. At the end of the reaction, particles were pelleted and the supernatant was collected for the evaluation of the coupling efficiency. Particles were washed three times with PBS, 0.1% Tween and stored in PBS, 0.01% Tween at 4˚C. Non-coupled anti-LIBS-LPETG was quantified by SDS-PAGE. The overall particle coupling procedure is summarized in figure 1b.

Conjugation of anti-LIBS-LPETG to 1 µm tosylactivated iron-oxide particles

10 mg particles were washed twice with 300 µl coating buffer (0.1M sodium borate, pH 9.5) each time. Particles were resuspended in 140 µl coating buffer and 27 µl of 15 mg/ml Boc-NH-linker-NH2 peptide and 83 µl of 3 M ammonium sulphate were added. After incubation for 16-24 hours at 37°C with shaking, 250 µl of blocking buffer (PBS, pH 7.4, 0.5% BSA and 0.05% Tween 20) was added and the mixture was incubated at 37°C overnight with shaking. After being washed three times with washing buffer (PBS, pH 7.4, 0.1% BSA, 0.05% Tween 20) and then 2 times with deionized water, the particles were resuspended in 100 µl of 50% trifluoroacetic (TFA) in dichloromethane (DCM) and incubated for 30 min with shaking at room temperature to de-protect the amine groups of the conjugated peptide (de-Boc). After washings, the particles were incubated with 10% triethanolamine (TEA) in DCM at room temperature for 20 min. Particles were then washed twice with water, twice with DMSO and resuspend in 173 µl DMSO. 27 µl of 15 mg/ml BocHN-GGGWW-OH peptide and 50ul of ByPOP/DIPEA/DMSO (2mg/1mg/100ul) were added. After being incubated at room temperature for 2 hours, particles were washed 3 times with water. Particles were incubated with 100 µl of 50% TFA/DCM for 30 minutes at room temperature with shaking. After 3 times washing with water, particles were incubated with 200 µl of 10% TEA/DCM for 20 min at room temperature with shaking. Then they were washed twice with water and twice with Sortase coupling buffer. 5 mg particles were resuspended in 300 µl of coupling buffer containing 20 µmol/L anti-LIBS-LPETG, 10 µmol/L Sortase A enzyme and 0.5 mmol/L CaCl2. The reaction mixture was incubated at 37˚C for 3 hours with shaking. Particles were then washed three times with washing buffer and stored in PBS, pH 7.4, 0.1% BSA, 0.05% Tween 20.

Isolation of mononuclear cells from human cord blood

Human cord blood was obtained from healthy donors following normal full-term deliveries after their written informed consent and kindly provided by Dr M. Lappas from the Department of Obstetrics and Gynecology, Mercy Hospital for Women, University of Melbourne. Ethics approval was granted by the Human Research Ethics Committee, Mercy Health, Mercy Hospital for Women, Melbourne, Australia. Cord blood was diluted 3 times

with isolation buffer (PBS without Ca/Mg, 0.1% BSA, 0.6% citrate, pH 7.4). 35 mL of diluted cord blood was layered on 15 mL of Ficoll-Paque™ Plus (GE Healthcare) in 50 mL Falcon tubes. After centrifugation at 800 xg (without brake and acceleration) for 20 min, the interphase containing mononuclear cells was collected and an equal volume of isolation buffer was added. The mixture was centrifuged at 500 xg (with brake and acceleration) for 20 min. The pellet was collected and resuspended in ACK lysis buffer (GIBCO, Invitrogen) according to manufacture's instructions. After incubation at room temperature for 10 min, 40 mL of isolation buffer was added to 10 mL of cell suspension and the mixture was centrifuged at 400 xg for 10 min. Cell pellet was collected and used in the next labelling study.

Labelling CHO cells and mononuclear cells (MNC) with anti-LIBS-LPETG

Anti-LIBS-LPETG scFv was coupled onto the cell surface by two methods. In the first method only one step (step 3) was used. In the second method, three steps were employed. Steps 1-3 are detailed below. The overall cell coupling procedures is summarised in figure 1c.

(1) Introduction of sulfhydryls to cell surface via reaction with primary amines using 2-Iminothiolane or Traut's reagent: CHO cells were trypsinized and washed once with PBS (without Ca and Mg). MNC cells were collected and washed once with PBS (without Ca and Mg). 1 x 10^6 cells were resuspended in 200 µl of modified PBS buffer with EDTA (PBS without Ca and Mg, 4500 mg/l glucose, 15 mmol/L HEPES, 2 mmol/L EDTA, pH 7.3). Traut's reagent was added at the final concentration of 0.6 mmol/L (16 µg). Cells were incubated for 30 min at room temperature with shaking. After the incubation, cells were washed once with modified PBS with EDTA.

(2) Labelling cells with NH_2-GGG- tags via specific reaction of sulfhydryls on cell surface and maleimide groups on NH_2-GGG-maleimide peptides: 1 x 10^6 cells were resuspended in 200 µl of modified PBS buffer with EDTA. NH_2-GGG-maleimide peptide was added to the final concentration of 12 µmol/L (2 µg). The reaction mixture was incubated for 30 min at room temperature with shaking. Cells were then washed once with modified PBS buffer without EDTA (PBS with Ca, Mg, 4.5 g/l glucose, 15 mmol/L HEPES, pH 7.3).

(3) Sortase-mediated coupling between anti-LIBS-LPETG and NH_2-GGG- groups on cell membrane: 1 x 10^6 cells were resuspended in 100 µl of modified PBS buffer without EDTA. Anti-LIBS-LPETG and Sortase A enzyme were added to the final concentration of 10 µmol/L and 10 µmol/L, respectively. Cells were incubated at 37˚C for 1 hour with shaking, then pelleted and washed twice with PBS. Since 50 mM Tris in Sortase coupling buffer significantly decreased the viability of cells, modified PBS buffer was used instead of Tris buffer in the Sortase conjugation step. The supernatant was collected for evaluation of the coupling efficiency. Non-coupled anti-LIBS was quantified by SDS-PAGE.

To optimise parameters in steps 1 and 2 (concentration of Traut's reagent, reaction buffer and incubation time), near-infrared (NIR) DyLight 800 maleimide was used instead of NH_2-GGG-maleimide peptide. The NIR intensity of the cells was analyzed after the conjugation process using Odyssey (LI-COR Biosciences). The optimum parameters (as detailed above) were chosen based on the efficiency of the conjugation and the viability of the cells (data not shown). To determine the concentration of NH_2-GGG-maleimide peptide in step 2 and to optimise step 3, enhanced green fluorescence protein with the LPETG motif (eGFP-LPETG) was used in the third step instead of anti-LIBS-LPETG. Flow cytometry was employed to assess coupling efficiency to cells. The optimal concentration of GGG-maleimide peptide and the incubation time in step 3 were decided based on the coupling efficiency and the cell viability (data not shown).

Evaluation of the coupling efficiency (SDS-PAGE)

30 µl of each sample (remaining reaction mixture) and 6 µl of 5X reducing SDS loading buffer were added to 1.5-ml tube and denatured at 96˚C for 5 min. 36 µl of each sample was run on SDS-PAGE gel in SDS running buffer at 30 mA for 2 hours. The gel was then stained with Coommassie Brilliant Blue for 1 hour and subsequently destained for at least 12 hours

with Coommassie destaining solution. The gel was visualised and analysed using a BioRad Gel-Doc system with Quantity One software (Australia).

Flow cytometry

Blood from healthy volunteers taking no medication was collected by venepuncture, anticoagulated with citric acid and centrifuged at 150 g for 10 min at room temperature. The supernatant platelet rich plasma (PRP) was collected and diluted (1:20) with PBS with calcium and magnesium. Diluted PRP were either activated by 20 µmol/L ADP or non-activated and incubated with different concentrations of the coupled anti-LIBS-eGFP products for 10 min at room temperature. Samples were then fixed with 500 µl Cellfix (BD Bioscience, USA) and analyzed by FACS Calibur (BD Bioscience, USA).

Preparation of purified platelets

PRP was collected and acidified to the pH of 6.5 using Acid Citrate Dextrose solution B (ACD-B, trisodium citrate, 13.2 g/l; citric acid, 4.8 g/l; and dextrose 14.7 g/l). The resulting PRP was centrifuged at 720 g for 10 min at room temperature. The supernatant was discarded and the pellet was resuspended in modified HEPES-Tyrode's buffer (JNL buffer, 6 mmol/L dextrose, 130 mmol/L NaCl, 9 mmol/L $NaHCO_3$, 10 mmol/L tribasic Na citrate, 10 mmol/L Tris base, 3 mmol/L KCl, 2 mmol/L HEPES free acid, 0.81 mmol/L KH_2PO_4, 0.9 mmol/L $MgCl_2$), pH 6.5. The pH of JNL buffer was adjusted by ACD-B (38 mmol/L citrate acid anhydrous, 75 mmol/L sodium citrate, 136 mmol/L Dextrose). The mixture was then centrifuged at 500 g for 10 min at room temperature. After removing the supernatant, the pellet was resuspended and diluted 3 times in JNL buffer, pH 7.4. $CaCl_2$ was added to the final concentration of 1.8 mmol/L.

Static adhesion assays

Coupled eGFP: 35mm FluoroDishes (World Precision Instruments Inc) were coated with fibrinogen: 300 µl of a 30 ng/µL solution of fibrinogen was added to the bottom of each dish and incubated at 4˚C overnight. Dishes were then washed twice with 1mL PBS (Ca, Mg). 1mL 1% BSA was added and dishes were incubated at room temperature for 1 hour and then washed twice. During this incubation PRP was gel filtered to remove contaminating proteins by Sepharose resin (Sigma-Aldrich, Australia): 4 ml of Sepharose resin in a filtration column was washed 3 times with 5 ml PBS (Ca, Mg). 1 ml of PRP was applied to the column and the flow through was discarded. 1 ml of PBS (Ca, Mg) was then added to the column and 1 ml of the flow through was collected. This was diluted 5-fold with PBS (Ca, Mg) and ADP was added to a final concentration of 20 µM. 300 µl of the diluted solution of gel-filtered platelets was added to the fibrinogen coated dishes and incubated at 37˚C for 30 min and then washed twice. 200 µL of 10 ng/µL coupled scFv-eGFP and an equimolar amount of uncoupled GGG-eGFP (as negative control) was added to the dishes and incubated for 30 minutes at 37˚C. Dishes were washed twice and then fixed with 500 µL Cellfix. Fluorescent and DIC Images were taken directly from the dishes using a Zeiss Axio Observer Z1 at 600x magnification.

***Coupled Dynabeads*:** 300 µl of diluted purified platelets was added onto 10-mm glass coverslip in 24-well plate and 18 µmol/L ADP was added. After incubating at 37˚C for 20 min, coverslips were washed twice with PBS (Ca, Mg) and then blocked with 300 µl of 1% BSA in JNL buffer (pH 7.4). After 30-min incubation at 37˚C, coverslips were washed twice, removed and added into lying-down 5-ml glass tubes with the platelet-coating sides faced up. Under continuous rolling of the tubes, coverslips were incubated with predetermined numbers of either targeted particles (anti-LIBS coupled particles) or non-targeted particles (GGG-particles) in PBS with 0.5% BSA at room temperature for 10 min. Coverslips were then washed twice with PBS for 10 min and fixed with Cellfix. Images were taken at 200x and 400x magnification by an inverted microscope (IX81, Olympus) with digital B/W camera (XM10, Olympus) and Cell^P 1692 (AnalySIS Image Processing software). Binding particles were quantified using Image J software.

Coupled CHO cells: 100 µl of diluted purified platelets was added into each well of a 96-well plate and stimulated with 18 µmol/L ADP. After incubating at 37˚C for 20 min, wells were washed twice with PBS (Ca, Mg) and then blocked with 100 µl of 1% BSA in JNL buffer (pH 7.4) for 30 min at 37˚C. After washing twice, platelet-coated wells were incubated with predetermined numbers of either targeted cells (anti-LIBS coupled cells) or non-targeted cells (GGG-cells) in PBS with 0.5% BSA at 37˚C for 10 min. Wells were then washed twice with PBS and fixed with Cellfix. DIC/fluorescent images were taken 200x magnification by an inverted microscope (IX81, Olympus) with digital B/W camera (XM10, Olympus) and Cell^P 1692 (AnalySIS Image Processing software). Binding cells were quantified using Image J software.

Flow chamber assays

Glass capillaries (0.20 x 2.0 mm I.D., 10 cm in length, Vitrotubes^{TM}, USA) were coated with 42 µl of 100 µg/ml collagen-1 overnight at 4˚C. Capillaries were then blocked with 1% BSA in PBS for 1 hour at 37˚C. Blood was taken from healthy donors, citrated and perfused through the capillary at a shear rate of 100 s^{-1}. After 5 min, thrombi with desirable sizes formed. The capillary was then washed by perfusing with PBS (Ca, Mg) for 5 min at a shear rate of 500 s^{-1} until no blood cells were observed. Particles or CHO cells in PBS containing 0.5% BSA (3 x 10^6 particles or cells/ml) was perfused through capillary for 5 min at different shear rates. Movies and images were taken at 200x magnification using inverted microscope (IX81, Olympus) with digital B/W camera (XM10, Olympus) and Cell^P 1692 (AnalySIS Image Processing software). Capillaries were washed with PBS and thrombi were specifically stained with FITC-PAC-1 or CD62P-PE. Binding particles and cells were quantified using Image J software. Thrombus area was estimated by Image-Pro Plus 6.0.

Staining of CHO cells

CHO cells within 20 passages were cultured in 175-cm^2 flask until they reached approximately 95% of confluency. The medium was removed and cells were washed once with PBS. CellTracker^{TM} Green CMFDA (Invitrogen, Australia) dye working solution (4 µmol/L in plain DMEM buffer without serum) was added to the flask containing the adherent cells. After incubating for 40 min at 37˚C/5% CO_2, the dye working solution was replaced with fresh and prewarmed plain DMEM medium (without serum). The cells were incubated for another 30 min at 37˚C/5% CO_2. They were then trypsinized, harvested and washed once with PBS before undergoing the coupling process.

Intravital studies

4-5 week old C57BL/6 wild-type mice weighing 15-17 g were anaesthetized by intraperitoneal injection of a ketamine:xylazine mixture (100:20 mg/kg body weight). Mesenteric arteries/veins (diameters 100-150 µm) were observed with inverted microscope (IX81, Olympus) and the images were recorded with digital B/W camera (XM10, Olympus). The injury of arteries/veins was induced by the micro-drop of 10% $FeCl_3$. When the thrombus started building up, 200 µl of PBS containing the predetermined amounts of particles or CHO cells was injected into the blood flow system via a jugular vein cannula. DIC and fluorescence images of the thrombus were taken before, during and after the injection at 200x magnification using an inverted microscope (IX81, Olympus) with digital B/W camera (XM10, Olympus) and Cell^P 1692 (AnalySIS Image Processing software). Particles were seen by their TRITC autofluorescence and CHO cells were visualized by CellTrackerTM Green CMFDA dye.

***In vitro* MRI experiments**

Blood from healthy volunteers taking no medication was anti-coagulated with citric acid and centrifuged at 1000 rpm for 10 min. Of the resulting platelet rich plasma, 1 mL was incubated with 88 µl Actin (Dade Behring) and 25 µl of 1M CaCl2 to induce coagulation. Anti-LIBS-MPIOs were added before thrombus formation or after the thrombus had been formed. Samples were incubated for 12 min at 37°C in a water bath, the developed clots were then

incubated with anti-LIBS-MPIOs and finally stored for another 30 min at 37ºC ambient temperature under continuous rotation. Clots were extensively washed with PBS and transferred into 2% low melting point agarose (Sigma). MRI of agarose-embedded clots was performed on a 4.7 Tesla scanner (Bruker, Germany). The embedded thrombi were placed within a MRI coil, having the longitudinal axes of the cone-shaped clots orientated horizontally and perpendicular to B0. A susceptibility-sensitive 3D FLASH sequence with TE/TR 9.1 ms/700 ms was run with a Matrix of 72x512x512 leading to a resolution of 130x130x150 µm.

***In vivo* MRI experiments and histology**

In vivo MRI experiments were conducted at the University of Freiburg (Freiburg, Germany). Care and use of laboratory animals followed the national guidelines and were approved by the institutional animal care and ethics committees of the University of Freiburg. 11-week old C57BL/6 wild-type mice weighing 24 g were anaesthetized by intraperitoneal injection of a ketamine:xylazine mixture (100:20 mg/kg body weight). Carotid arterial wall-adherent thrombosis was induced with 6% ferrous chloride. Animals were transferred to the MRI system (94/20 Bruker BioSpec, Bruker, Germany) and were connected to an ECG and breathing-rate monitor and placed in the animal bed. Vital signs were monitored throughout the entire experiment, and body temperature was supported by a warm-water tube integrated in the animal bed. Anesthesia was continuously switched from ketamine to 1% to 1.6% isoflurane in O2 starting with a heart rate rising above 190 bpm and maintaining a breathing rate of 60"20 breaths per minute. During the complete measurement, mice were placed in the center of a quadrature whole-body birdcage resonator (35 mm inner diameter). Imaging consisted of a pilot scan with 3 orthogonal slices followed by a respiration-gated coronal 2-dimensional gradient-echo sequence oriented parallel to the oesophagus with an echo time (TE) of 4.4 ms, a repetition time (TR) of 250 ms, a flip angle of 40°, and a field of view of 25x25 mm. Via the coronal images, a volume (27x27x7.5 mm), including the bifurcation and the upstream carotid arteries beyond the lesion, was planned for the 3-dimensional (3D) gradient-echo sequence, monitoring the wall-adherent thrombosis. This 3D fast low-angle shot (FLASH) sequence had a TE of 2.8 ms, a TR of 20 ms, a bandwidth of 55 kHz, and an asymmetric echo with an echo position of 25%; a flip angle of 15° was chosen to gain good contrast between blood and surrounding tissue. With a matrix of 256x256x96, a resolution of 105x105x78 µm per pixel was achieved at a total acquisition time of 12 min 17 se. After a baseline 3D volume was acquired, mice were injected via a tail vein catheter with the anti-LIBS-MPIO ($4x10^8$ MPIOs) in a total volume of 200 µL saline. The 3D FLASH sequence was then repeated with equal parameters and geometry. MRI scans were performed continuously for up to 50 min.

After in vivo MRI was performed, animals were deeply anesthetized with ketamine and xylazine. Transcardiac perfusions via the left ventricle were carried out with saline. The injured carotid artery was removed, embedded in optical coherence tomography TissueTec (Sakura Finetec, Loeterwoude, the Netherlands), and frozen for histology. For the detection of wall-adherent thrombosis by histology, mouse platelets were detected with rat anti-mouse GPIIb (CD41) polyclonal antibody (Clone MWReg30, GeneTex, Inc, San Antonio, Tex); primary antibody was detected with a rabbit anti-rat biotinylated secondary antibody (Vectastain ABC-AP Kit, Vector, Loerrach, Germany) and VectorRed (Vector, Germany).

Statistical analysis

Results are presented as mean ± SD. Data were analyzed for statistical significance using 1-tailed paired t-test. The data was checked for normal distribution by Kolmogorov–Smirnov normality test. Where normal distribution could not be detected, a non-parametric Mann Whitney 1-tailed test was applied. A probability value (P) ≤ 0.05 was considered significant.

SUPPLEMENTAL FIGURES AND FIGURE LEGENDS

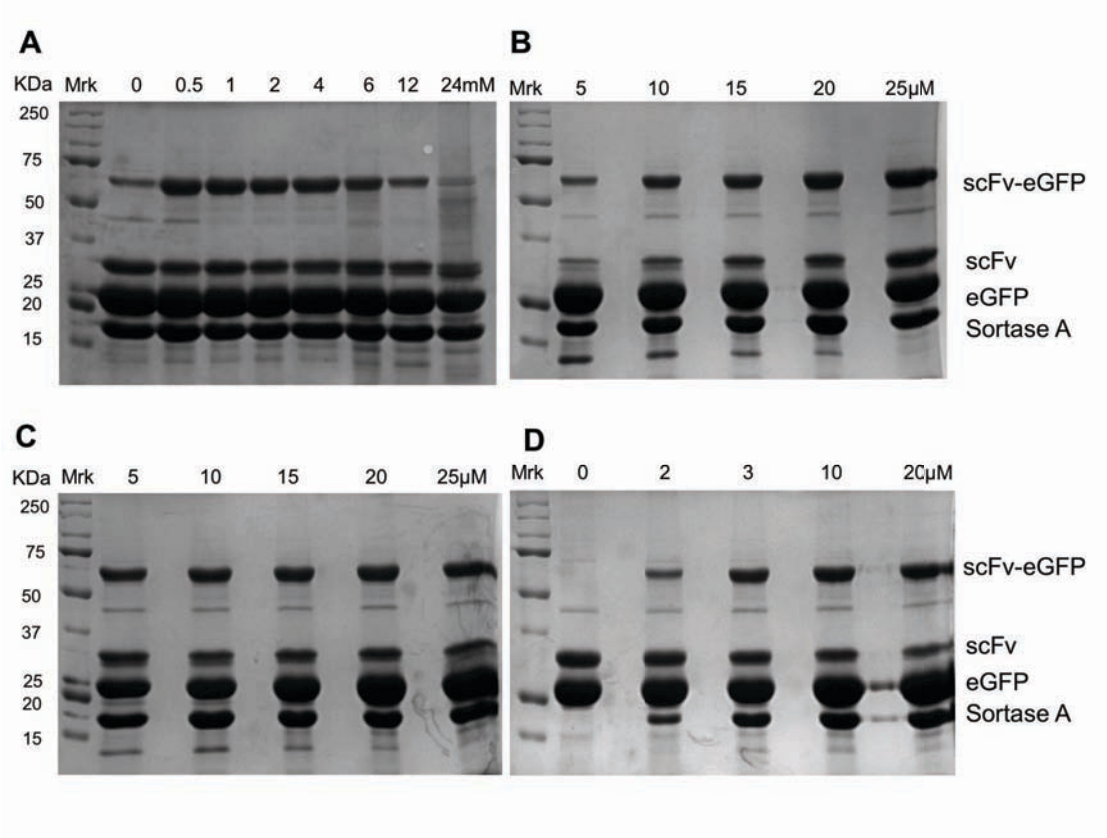

Online figure I: SDS-PAGE gels showing the effects of increasing concentrations of (A) $CaCl_2$, (B) scFv, (C) eGFP, and (D) Sortase A on the formation of the coupled product (scFv-eGFP). Mrk: protein marker.

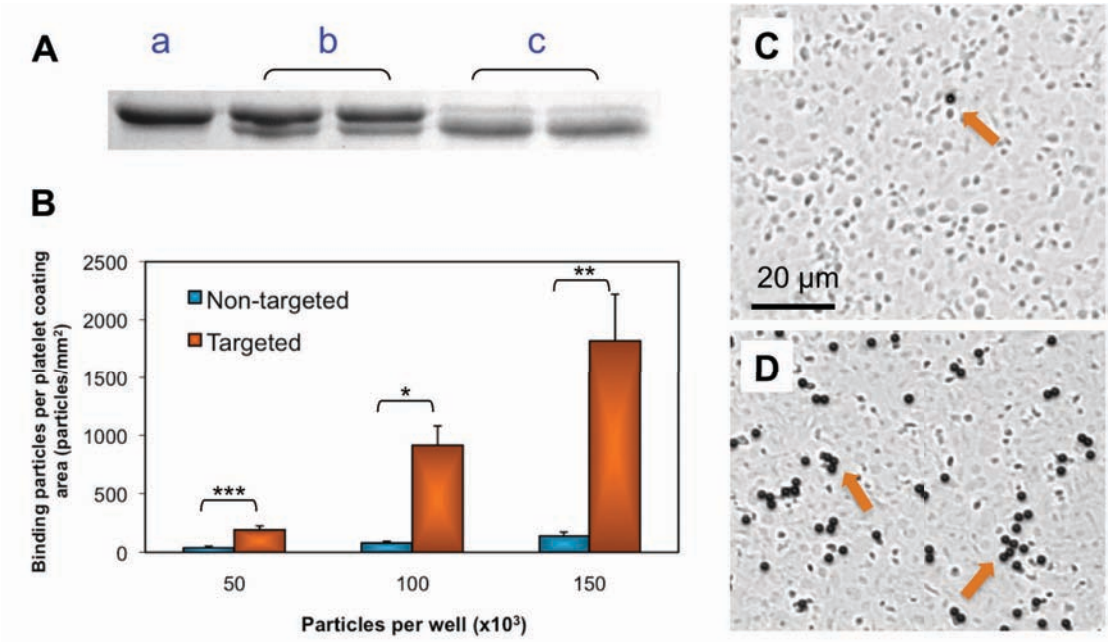

Online figure II: Successful scFv-particle coupling reaction and specific binding of coupled particles to activated platelets coated cover slips. (A) After the coupling reaction, particles were pelleted and the remaining reaction solutions were analysed via SDS-PAGE electrophoresis. a, b and c represent scFv from the control solution (scFv alone), the reaction mixture without Sortase A, and the complete reaction mixture, respectively. (B) Number of particles binding to activated platelets. Specific binding of scFv-coupled MRI particles is clearly demonstrated (*$P < 0.05$, **$P < 0.0005$, n=6, 1-tailed paired t-test). (C) and (D) Binding of specific (scFv-coupled) and non-specific (control) particles onto the layer of activated platelets where 100,000 particles were incubated in each well (*particles*: round black objects, pointed by orange arrows; *platelets*: gray colour, various sizes and shapes).

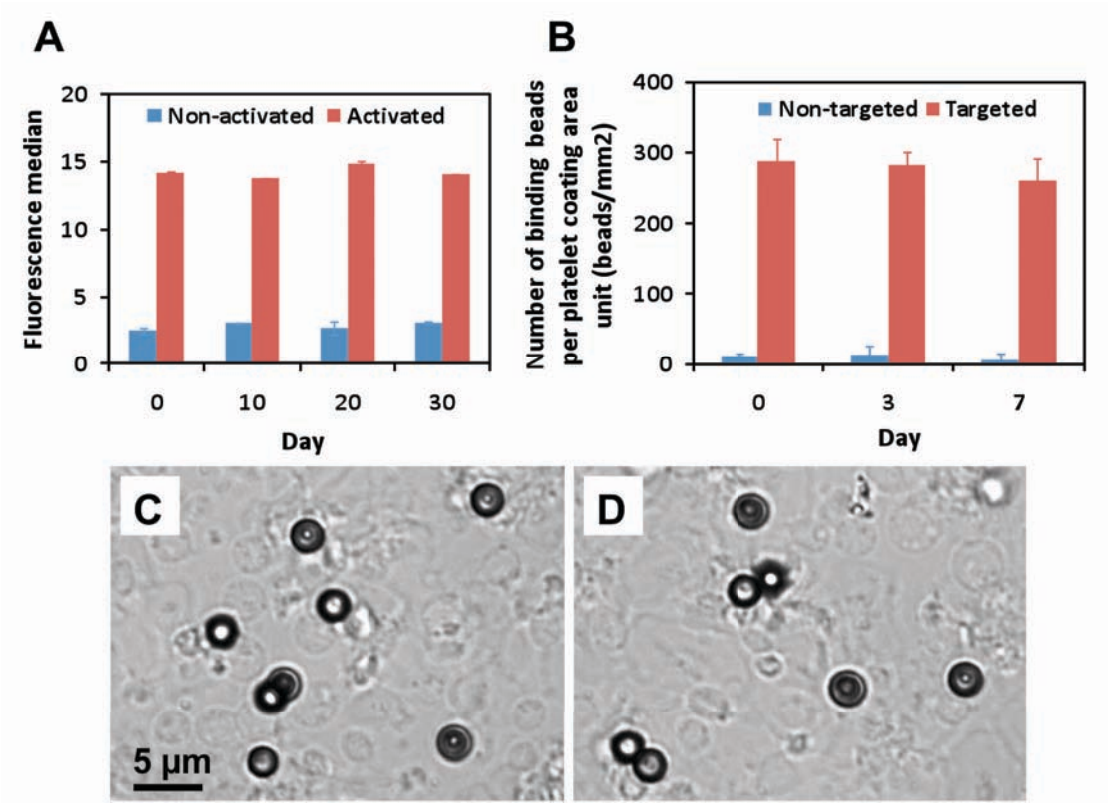

Online figure III: Stability of anti-LIBS scFv and scFv-conjugated particles at 4°C. (A) Graph showing the preserved binding of anti-LIBS scFv to activated platelets in flow cytometry setting. (B) Graph showing the preserved binding of targeted particles to activated platelets coated cover slips (n=3). (C) and (D) Binding of targeted particles onto the layer of activated platelets on day 0 and day 7, respectively (*particles*: round black objects; *platelets*: gray colour, various sizes and shapes).

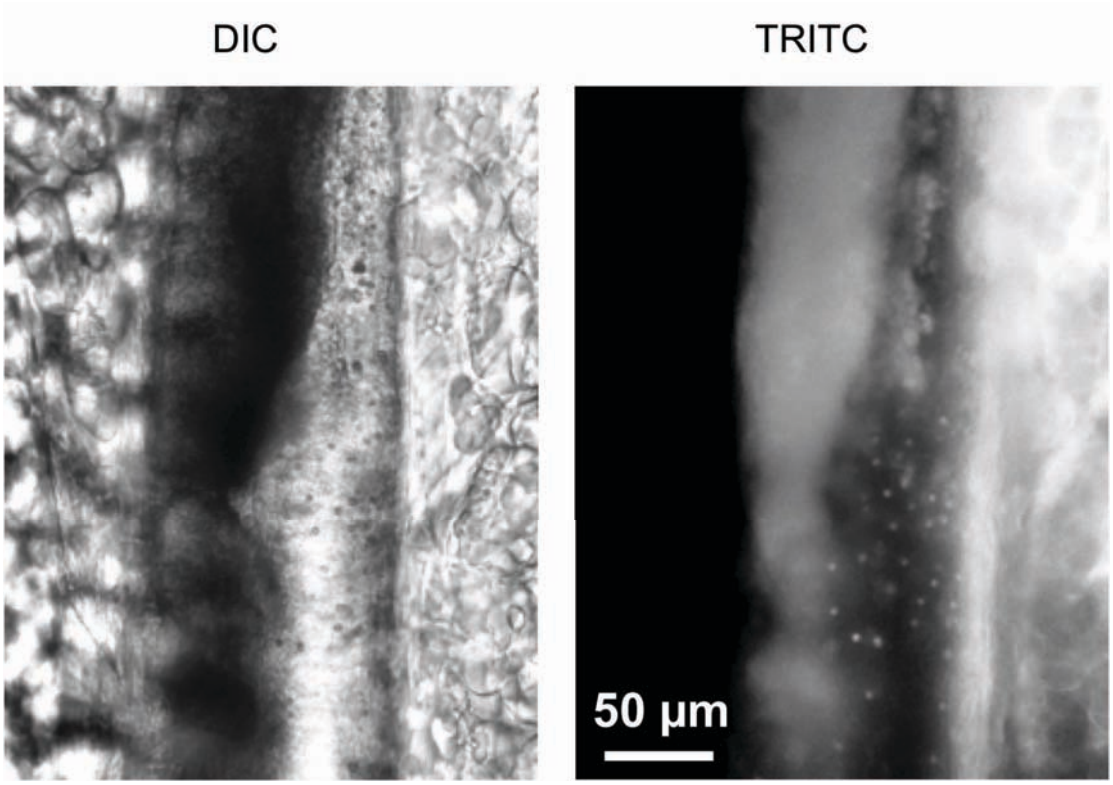

Online figure IV: Binding of scFv-particles to a growing thrombus resulting in the incorporation of the particles within the thrombus.

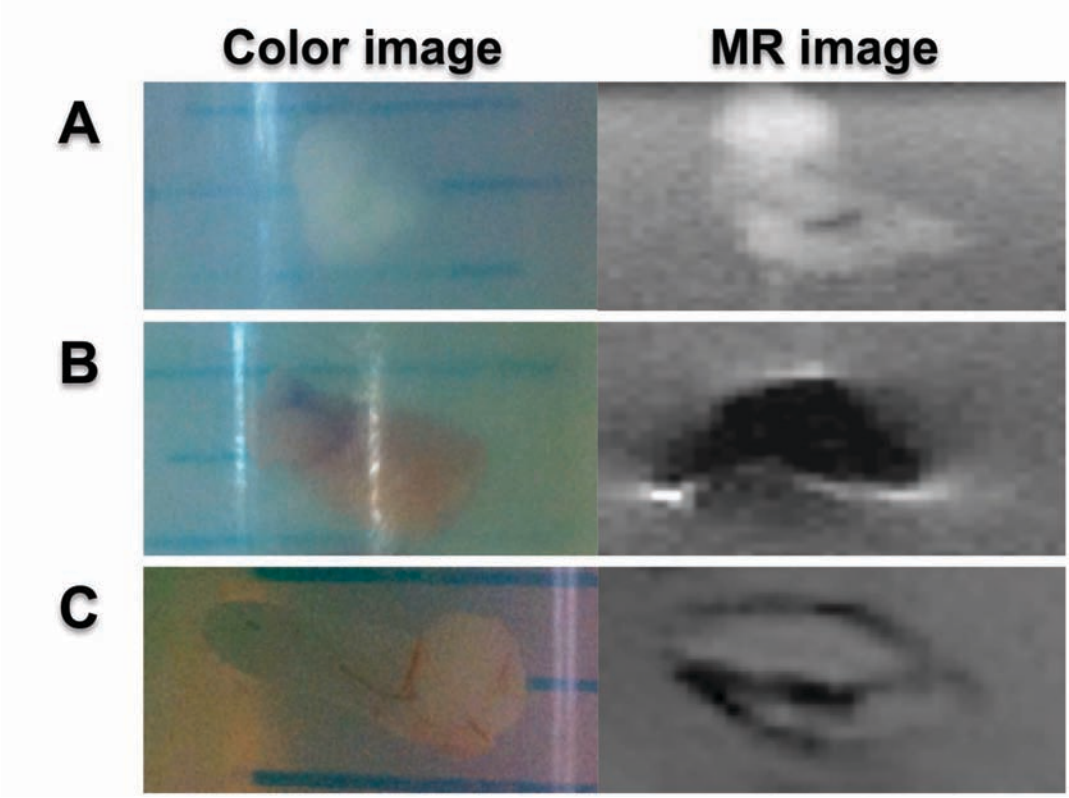

Online figure V: Color and MR images of a blank thrombus (A), a thrombus with MPIOs incorporated within (B) and a thrombus with MPIOs binding on its surface (C).

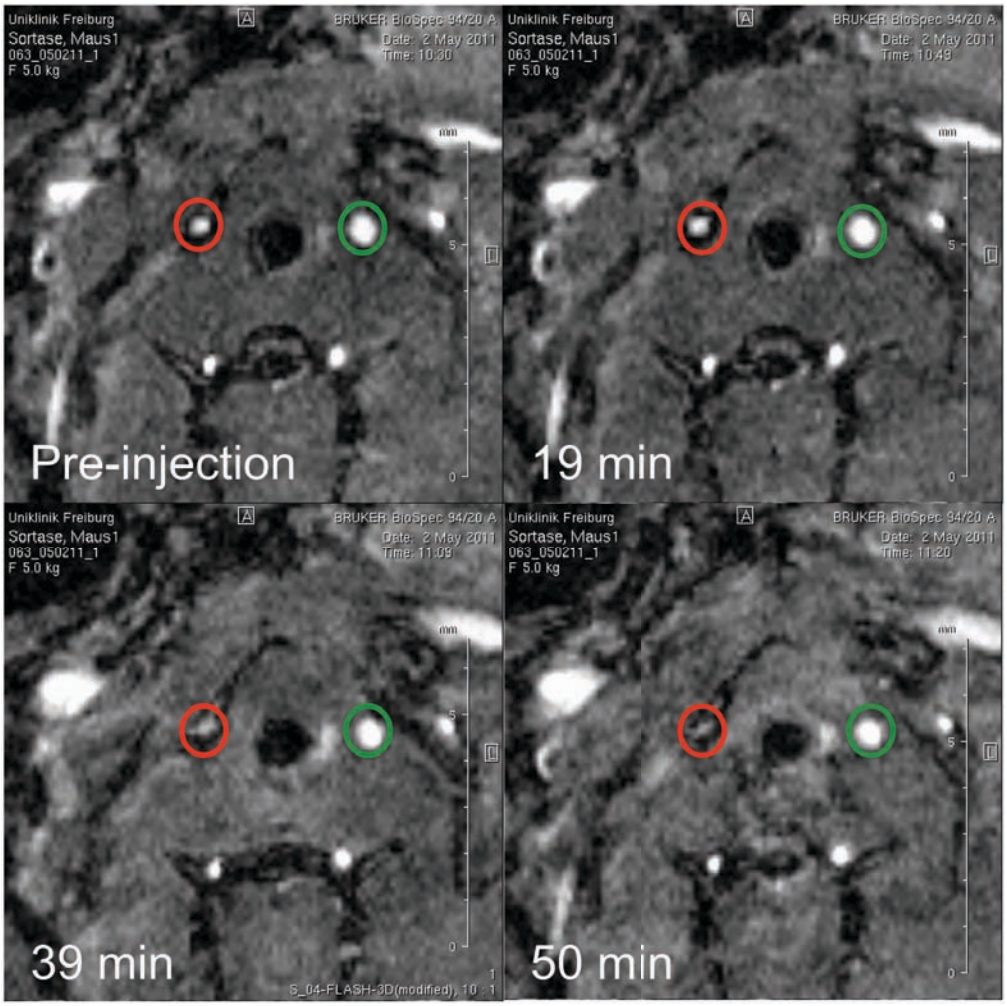

Online figure VI: Transverse sections showing in vivo MRI after carotid artery injury. Right carotid artery was injured (red circle) and left carotid artery was non-injured (green circle). After injection of anti-LIBS-MPIOs, there was increasing signal drop at 19, 39 and 50 minutes compared with pre-injection image and the non-injured left carotid artery. This represents the typical susceptibility artefact caused by MPIOs in T2*-weighted MRI and indicates anti-LIBS-MPIOs binding.

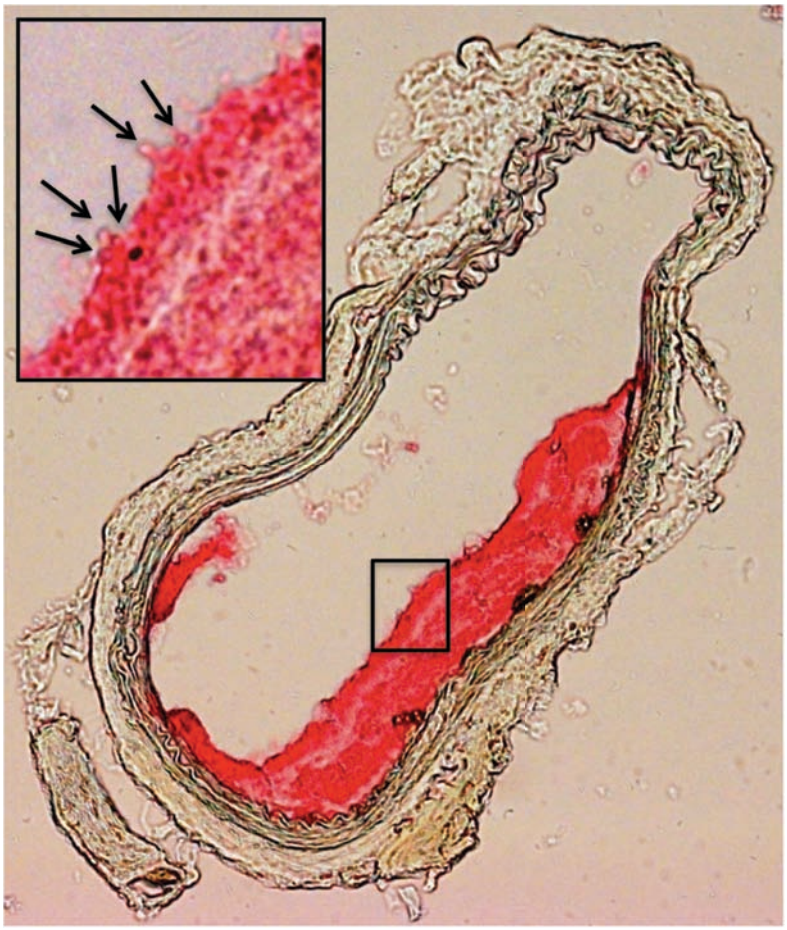

Online figure VII: Immunohistochemistry of a wall-adherent thrombus in anti-LIBS MPIO–injected animal. In the inlet, arrows depict the typical appearance of bound MPIOs on the thrombus surface in frozen sections; the thrombus area itself appears red in Immunohistochemistry (anti-CD41 staining).

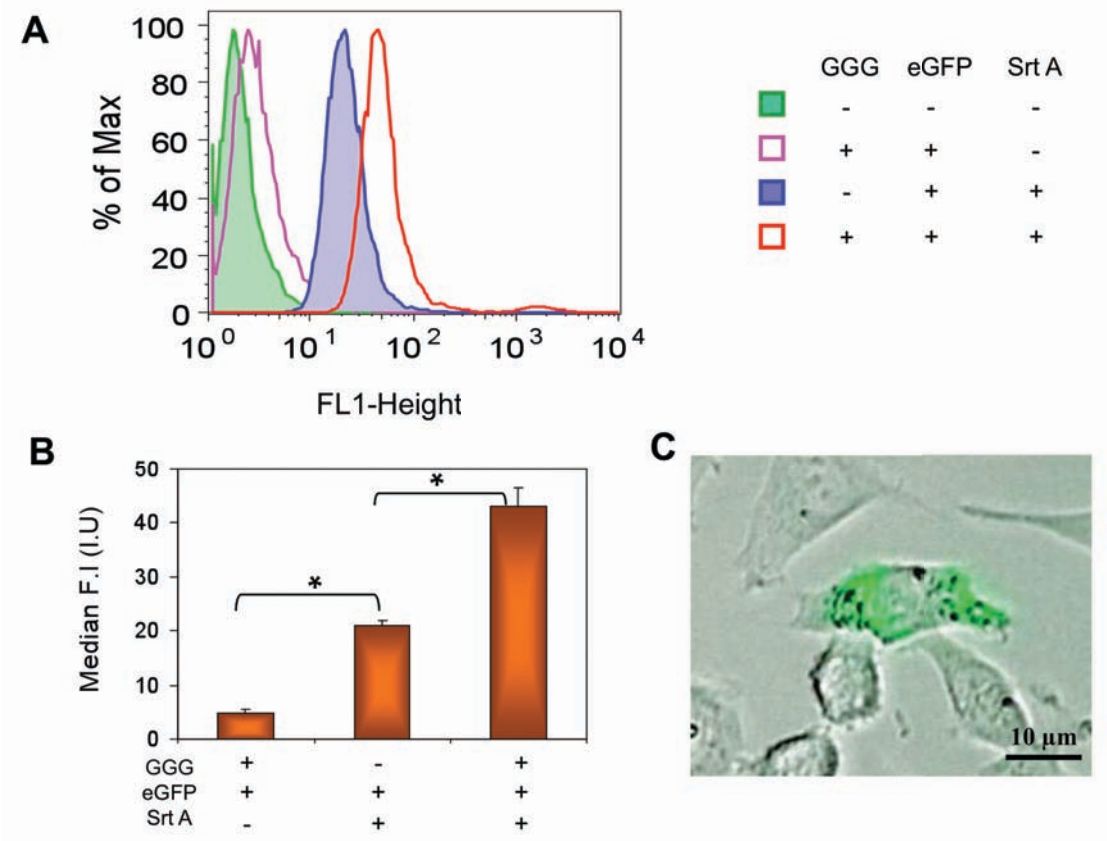

Online figure VIII: Labelling eGFP onto CHO cell surfaces as proof of concept for the coupling of scFv onto cells. (A) CHO cells chemically tagged with GGG motif and fused to eGFP-LPETG under the catalytic activity of Sortase A were analyzed in flow cytometry. (B) Graph summarizing the data from A and representing the median fluorescence intensity of CHO cells after the reaction (*P < 0.05, n = 4, Mann Whitney 1-tailed test). (C) Merged image demonstrating CHO cell with eGFP labelled on the surface.

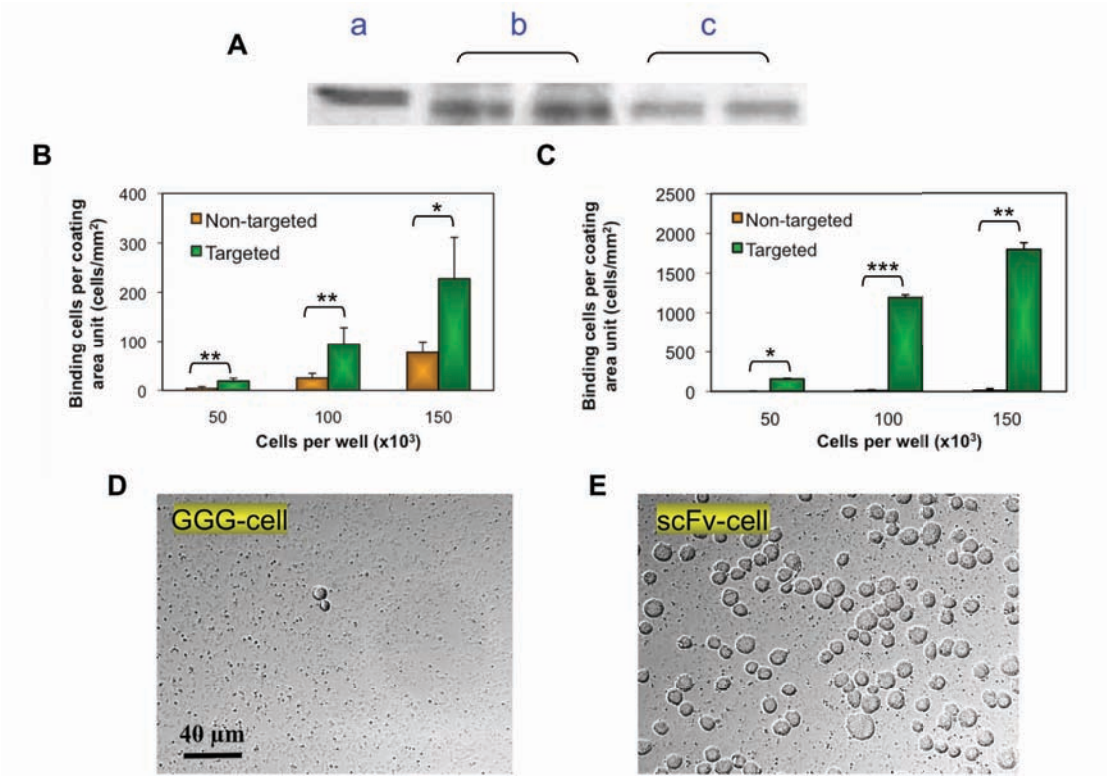

Online figure IX: Successful coupling reaction between CHO cells and scFv, and specific binding of scFv-coupled cells to activated platelets immobilized on coverslips. (A) After the coupling reaction, cells were pelleted and the remaining reaction solutions were analyzed via SDS-PAGE electrophoresis. a, b and c represent scFv from the control solution (scFv alone), the reaction mixture in protocol A, and the reaction mixture in protocol B, respectively. (B) and (C) Number of cells (prepared by protocol A and B, respectively) binding to activated platelets. There is a significant specific binding of scFv-coupled cells to a layer of activated platelets (*$P < 0.01$, **$P < 0.005$, ***$P < 0.0001$, n=6, 1-tailed paired t-test). The numbers of bound scFv-cells were significantly higher than those of control (GGG-) cells in both protocols. Protocol B exhibited a more efficient procedure for cell coupling as demonstrated by the much higher number of coupled cells binding to the coating platelets. (D) and (E) Binding of non-targeted (GGG-) and targeted (scFv-coupled) cells (green arrows) prepared by protocol B to coating platelets (orange arrows) where 100,000 cells were incubated in each well.

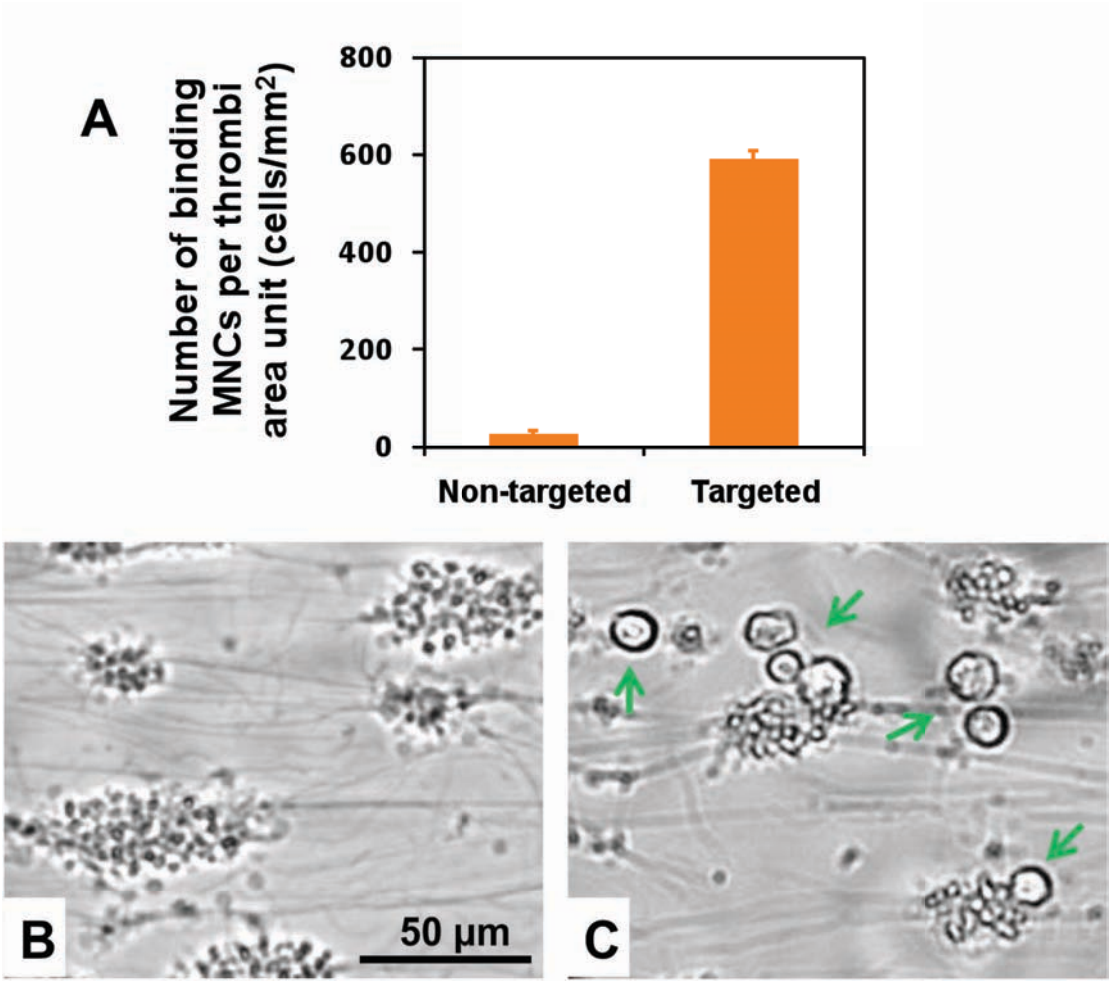

Online figure X: Targeting of scFv-coupled mononuclear cells to platelet aggregates under shear rate (250 s^{-1}) in a flow chamber system after 5 min. (A) Graph showing number of non-targeted cells (GGG-cells) and targeted cells (scFv-cells) binding to thrombi ($P < 0.05$, n=3, Mann Whitney 1-tailed test) after 5 min perfusion. (B) and (C) Images showing the binding of non-targeted and targeted cells on platelet aggregates, respectively (cells are pointed by green arrows). Platelet aggregates formed by the aggregation of activated platelets on collagen-1 fibres immobilized on the chamber surface.

SUPLLEMENTAL REFERENCES

1. Stoll P, Bassler N, Hagemeyer CE, Eisenhardt SU, Chen YC, Schmidt R, Schwarz M, Ahrens I, Katagiri Y, Pannen B, Bode C, Peter K. Targeting Ligand-Induced Binding Sites on GPIIb/IIIa via Single-Chain Antibody Allows Effective Anticoagulation Without Bleeding Time Prolongation. *Arterioscler. Thromb. Vasc. Biol.* 2007;27:1206-1212.

2. Schwarz M, Katagiri Y, Kotani M, Bassler N, Loeffler C, Bode C, Peter K. Reversibility and persistence of GPIIb/IIIa blocker-induced conformational change of GPIIb/IIIa (CD41/CD61). *J. Pharmacol. Exp. Ther.* 2004;308:1002-1011.

3. Han K. An efficient DDAB-mediated transfection of Drosophila S2 cells. *Nucleic Acids Res.* 1996;24:4362-4363.

4. Ton-That H, Liu G, Mazmanian SK, Faull KF, Schneewind O. Purification and characterization of sortase, the transpeptidase that cleaves surface proteins of Staphylococcus aureus at the LPXTG motif. *Proc. Natl. Acad. Sci. USA.* 1999;96:12424-12429.

5. Parthasarathy R, Subramanian S, Boder ET. Sortase A as a novel molecular "stapler" for sequence-specific protein conjugation. *Bioconjug. Chem.* 2007;18:469-476.

LEGENDS FOR VIDEO FILES

Supplemental Video 1: Binding of control GGG-particles to thrombi under a shear rate of 500 s^{-1} in a flow chamber setting.

Supplemental Video 2: Binding of anti-LIBS-particles to thrombi under a shear rate of 500 s^{-1} in a flow chamber setting.

Supplemental Video 3: Binding of control GGG-particles to ferrous chloride-induced thrombus in mouse messenteric artery.

Supplemental Video 4: Binding of anti-LIBS-particles to ferrous chloride-induced thrombi in mouse messenteric artery.

Supplemental Video 5: Binding of control GGG-CHO cells to thrombi under a shear rate of 100 s^{-1} in a flow chamber setting.

Supplemental Video 6: Binding of anti-LIBS-CHO cells to thrombi at a shear rate of 100 s^{-1} in a flow chamber setting.

Supplemental Video 7: Binding of control GGG-CHO cells to a ferrous chloride-induced thrombus in a mouse messenteric vein.

Supplemental Video 8: Binding of anti-LIBS-CHOcells to a ferrous chloride-induced thrombus in a mouse messenteric vein.